CDAP-TR-045
for U.S. Nuclear Regulatory Commission

CODE DEVELOPMENT AND ANALYSIS PROGRAM

DEVELOPMENTAL CHECKOUT OF THE BEACON/MOD2A CODE

J. A. RAMSTHALER J. F. LIME
M. S. SAHOTA

NRC Research and Technical Assistance Report

December 1978

EG&G Idaho, Inc.

IDAHO NATIONAL ENGINEERING LABORATORY

DEPARTMENT OF ENERGY

IDAHO OPERATIONS OFFICE UNDER CONTRACT EY-76-C-07-1570

EG&G Idaho, Inc

FORM EG&G 398
(Rev 12-78)

INTERIM REPORT

Accession No. ____________

Report No. CDAP-TR-45

Contract Program or Project Title: Containment Analysis Development

Subject of this Document: Developmental Checkout of the BEACON/MOD2A Code

Type of Document: Status Report

Author(s): J. A. Ramsthaler, J. F. Lime, M. S. Sahota

Date of Document: December 1978

Responsible NRC Individual and NRC Office or Division: S. Fabic, Reactor Safety Research

> This document was prepared primarily for preliminary or internal use. It has not received full review and approval. Since there may be substantive changes, this document should not be considered final.

EG&G Idaho, Inc.
Idaho Falls, Idaho 83401

Prepared for the
U.S. Nuclear Regulatory Commission
and the U.S. Department of Energy
Idaho Operations Office
Under contract No. EY-76-C-07-1570
NRC FIN ^'

INTERIM REPORT

SUMMARY

A best-estimate transient containment code, BEACON, is being developed by EG&G Idaho, Inc. for the Nuclear Regulatory Commission's reactor safety research program. This is an advanced, two-dimensional fluid flow code designed to predict temperatures and pressures in a dry PWR containment during a hypothetical loss-of-coolant accident. The most recent version of the code, MOD2A, is presently in the final stages of production prior to being released to the National Energy Software Center.

As part of the final code checkout, seven sample problems were selected to be run with BEACON/MOD2A. This series of problems was run to verify that all models were working properly and that the code was basically error free. Each problem was designed to investigate different models, including four new code options, partial flow, variable mesh, wall film, and heat structures. The complexity of the problems chosen ranged from a simple one-region case to a mixed-dimensional, multi-region arrangement.

Presentation of the results of the checkout includes a diagram of each problem configuration, modeling description, card input listing, and plots of predicted velocity vectors, void fraction, temperatures, pressures, or film mass, where applicable.

The results of the calculations were analyzed qualitatively and checked for reasonableness of the answers. The checkout indicates that all of the BEACON/MOD2A models appear to be handling physical phenomena correctly and that no gross errors are evident. This report documents the results of the code checkout prior public release.

CONTENTS

LIST OF FIGURES

TABLES

DEVELOPMENTAL CHECKOUT OF THE BEACON/MOD2A CODE

I. INTRODUCTION

The Code Development and Analysis Program of EG&G Idaho, Inc. is developing a transient containment code, BEACON, for the United States Nuclear Regulatory Commissions's reactor safety research program. This code is designed to predict fluid flow and resulting temperatures and pressures within a dry PWR containment building during a hypothetical loss-of-coolant accident (LOCA). Ultimately, predictions from computer codes such as BEACON will be used in the design, licensing, and safety analysis of future PWR power plants.

The most recent version of the code, BEACON/MOD2A, is a dynamic, two-component, two-phase, best estimate code which can be used to model relatively short-term transients during a LOCA. One- and two-dimensional or lumped parameter modeling of single- and multi-region complexes are all available. Non-equilibrium, two-phase phenomena can be simulated by utilizing the unequal velocity, unequal temperature features of the code. In addition, the inclusion of wall film and heat structure options in this version of the code allows for the modeling of heat transfer effects during longer transients.

BEACON/MOD2A[a] is scheduled to be publicly released to the National Energy Software Center at the end of 1978. As part of the checkout prerequisite to release, a series of seven sample problems was run to investigate the various models and options in the code. The first five problems had been used to check out earlier versions of BEACON. These were rerun, at this time, and compared with previous results to assure that no errors had been introduced into MOD2A. Two additional sample problems were created and run to check out the four new models in MOD2A; partial flow, variable mesh, wall film, and heat structures.

---

[a] A developmental version of BEACON/MOD2A (Configuration Control Number H00600IB) was used in the code checkout for this report. The released version of MOD2A should be identical to this version with the possible exception of minor coding corrections.

The purpose of this report is to document the results of running the seven checkout problems with BEACON/MOD2A. Results from each case are intended to provide a qualitative evaluation of the different options in the code. It was not intended that data comparisons would be made, however, reasonableness of the answers was ascertained in the checkout.

Each problem is presented with a brief description, modeling techniques, input listing, and plotted results in Section II. The conclusions and results of the checkout of BEACON/MOD2A are given in Section III.

II. SAMPLE PROBLEMS

A series of seven sample problems was selected to check out the various modeling features of the BEACON/MOD2A code. The problems range from a simple single-region example to the more complicated mixed-dimensional, multi-region setups. The first five problems have all been run before to check out previous versions of BEACON. They were rerun with MOD2A to insure that no errors were introducted into this new version of the code. The last two problems were designed specifically to check out the four new options developed for MOD2A, partial flow, variable mesh, wall film, and heat structures. The specific modeling features illustrated with each of the problems are noted in Table I.

The seven problems presented are:

(1) Single Eulerian region, closed boundaries

(2) Flow boundaries and obstacle cells

(3) Mixed dimensional, multi-region coupling

(4) Lumped parameter and unequal area coupling

(5) Source cell addition

(6) Partial flow

(7) Dry, multi-compartment containment with wall film and heat structures.

Each case is presented with a problem discussion, illustration of the configuration, and modeling description. The input data in card image form is also given.

Results for each problem are presented in the form of both plots and interpretive discussions. Vapor, liquid, and film velocity vector plots are shown, where applicable. Contour or time history plots of void fraction, pressure, temperature, and film mass are also given for various problems. Where the BEACON computer plots are presented, the legends are also included for interpretive purposes. For these plots, time is given in seconds, pressure in N/m^2, velocity in m/s, temperature in K, and film mass in kg.

The results are to be interpreted qualitatively rather than quantitatively, inasmuch as each problem was only intended to check out certain modeling features of the BEACON code and are not verification-type problems. In most cases, the expected flow phenomena and results are self-explanatory.

TABLE I

SAMPLE PROBLEM MODELING FEATURES

MODELING FEATURE	SAMPLE PROBLEM NUMBER 1	2	3	4	5	6	7
Cartesian Geometry		X	X	X	X	X	X
Axisymmetric Geometry	X						
Variable Mesh Spacing*							X
Flow Boundaries		X	X			X	
Obstacle Cells		X					
Partial Flow Cells*						X	
Source Addition					X		X
One-Dimensional Flow				X			X
Lumped Parameter				X			X
Mixed-dimensional, Multi-region Coupling			X	X			X
Wall Film*							X
Heat Structures*							X

* New option added for MOD2A.

1. SAMPLE PROBLEM 1: SINGLE EULERIAN REGION, CLOSED BOUNDARIES

This problem illustrates the use of the BEACON code with essentially the least number of modeling options exercised. It is therefore one of the more simple BEACON problems to set up. The problem models a rising slug of air in a circular tank as shown in Figure 1. At the initial problem time, an air bubble is released from the bottom of the tank and allowed to rise. The right-half of the circular cylinder is divided into an axisymmetric computing mesh. There are 7 cells radially from the centerline and 10 cells axially along the line of symmetry. The air bubble is formed by a 2 by 2 cell region at the lower left corner of the computing mesh. All of the boundaries are assumed rigid with free-slip.

A listing of the necessary input data is shown in Figure 2. The lefthand column of numbers lists the card number required to identify each input data card.

Plot output at a problem time of one second are presented to illustrate the resultant flow pattern. Vapor and liquid velocity vectors are shown in Figures 3 and 4, respectively. Void fraction and pressure gradients are shown in Figures 5 and 6, respectively.

The behavior of the problem is as expected. The air slug rises under the influence of gravity producing convection currents in the liquid. The rate of bubble rise is influenced by the interphasic momentum or drag force. In this example, the interphasic forces are modeled based on a dispersed or bubbly-type flow interaction. It is noted that in the time span computed, the vapor and liquid regions have become diffused. The diffusion occurs due to the lack of a sharp interface tracking capability in BEACON.

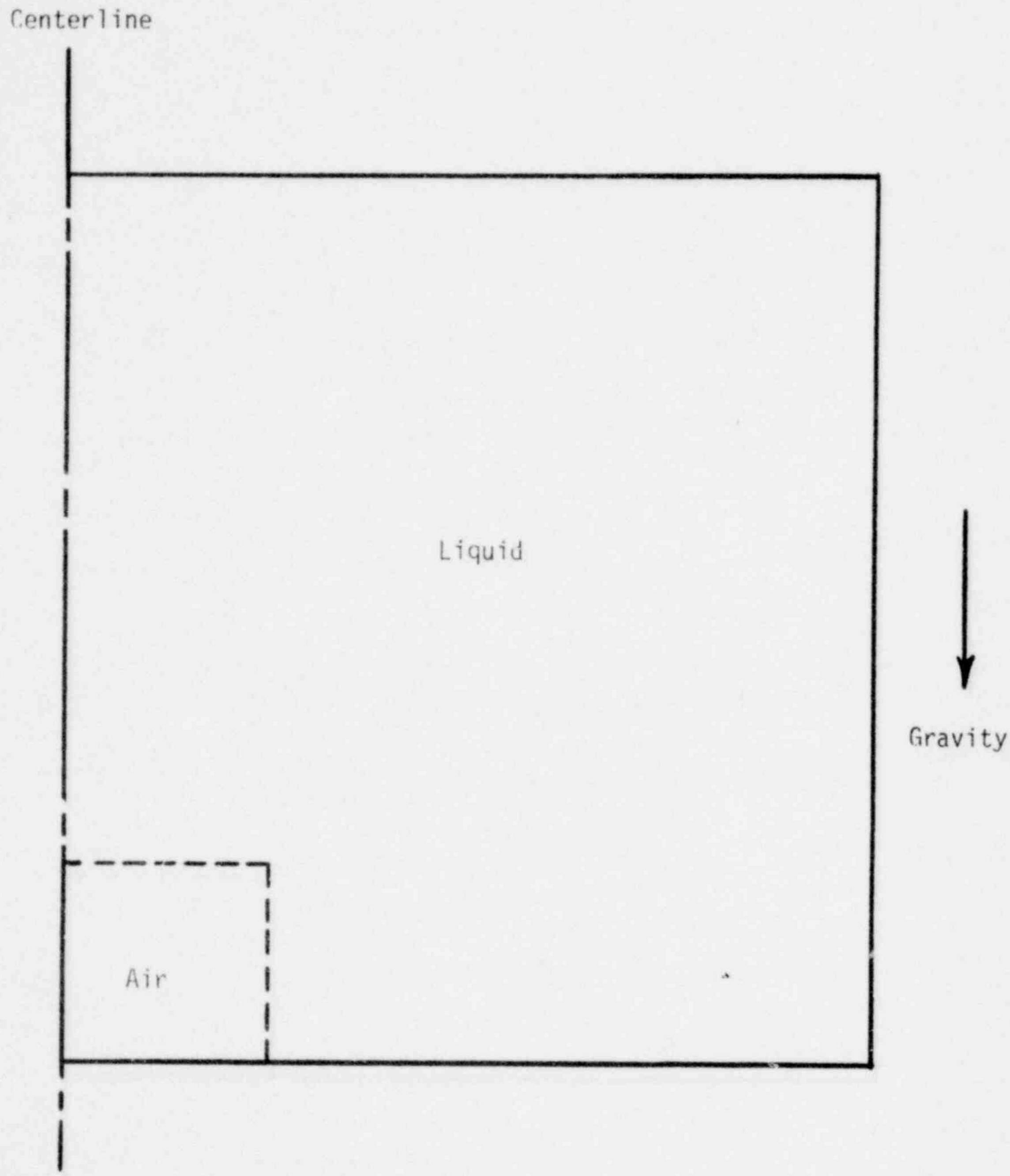

Fig. 1 Initial configuration for Sample Problem 1 before the air bubble has risen to the top of the liquid.

```
00100   'EXAMPLE PROBLEM 1:  SINGLE EULERIAN REGION, CLOSED BOUNDARIES'
************BASIC PROBLEM INPUT
00110   0.0, 1.0,    0.001, SEC, 2.0, 20, XEC
00120   0.001, 0.02, 0.002, 0.1, 0.005, 2.0
00130   AUTODT, 10, 0.1, 1.0E06
00140     PRINT, NOPRINT,    PRINT,   PRINT,   PRINT, 9999
00150     PLOTS, 0.9, 1 1 0 0 0 0 0 0 0 0 0 0
00200   1.5, 0.00001, 0.00001, 300, 5, 5
00210   -32.174, FT SEC-2, 0.020, 0.38, BTU/HR-FT-DEGF, 10000.0
00220   1.5E-04, 2.8E-06, FT2/SEC, 1.0, 1.0, MM, 23800.0, FT3, 1.0E04, 2
00230   0, 0.0, 0.0
00240   LASL, PT, N/M2, DEGK, M, SEC-1
************EULERIAN REGION INPUT
11000   AXISYM  7, 10, 1.0, 1.0, 0.0, FT, 0.0, 1.0
11010   SLIP, SLIP, SLIP, SLIP
11101   MIXTURE  2,2,3,3, 0, 1.0E05, 350.0, 350.0, 1.00, 1.0
11102   MIXTURE  4,2,8,3, 0, 1.0E05, 350.0, 350.0, 0.00, 1.0
11103   MIXTURE  2,4,8,11, 0, 1.0E05, 350.0, 350.0, 0.00, 1.0
.
```

Fig. 2 Input card listing for Sample Problem 1.

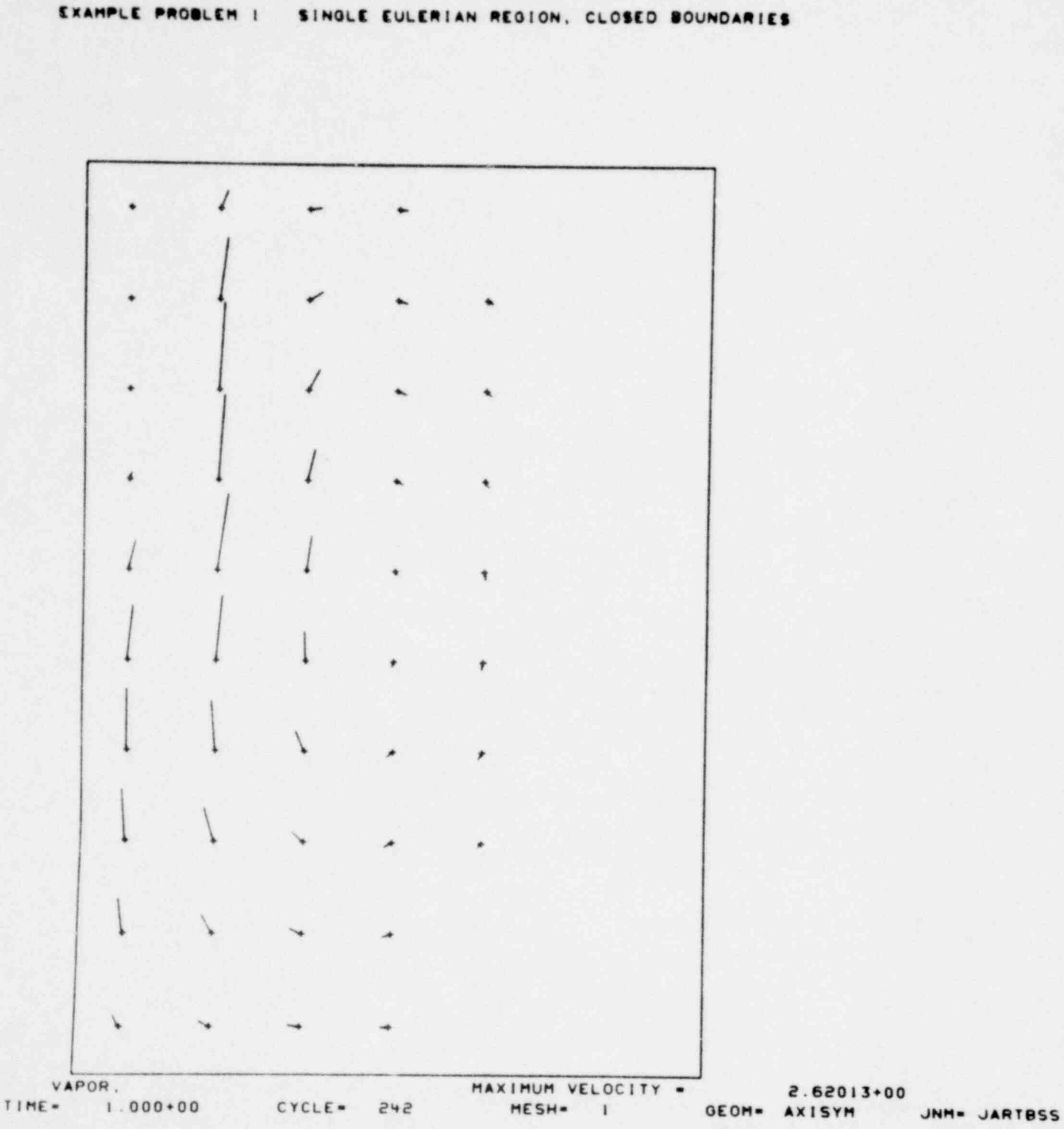

Fig. 3 Velocity vector plot for Sample Problem 1 showing the movement of the vapor in the liquid.

EXAMPLE PROBLEM 1 SINGLE EULERIAN REGION, CLOSED BOUNDARIES

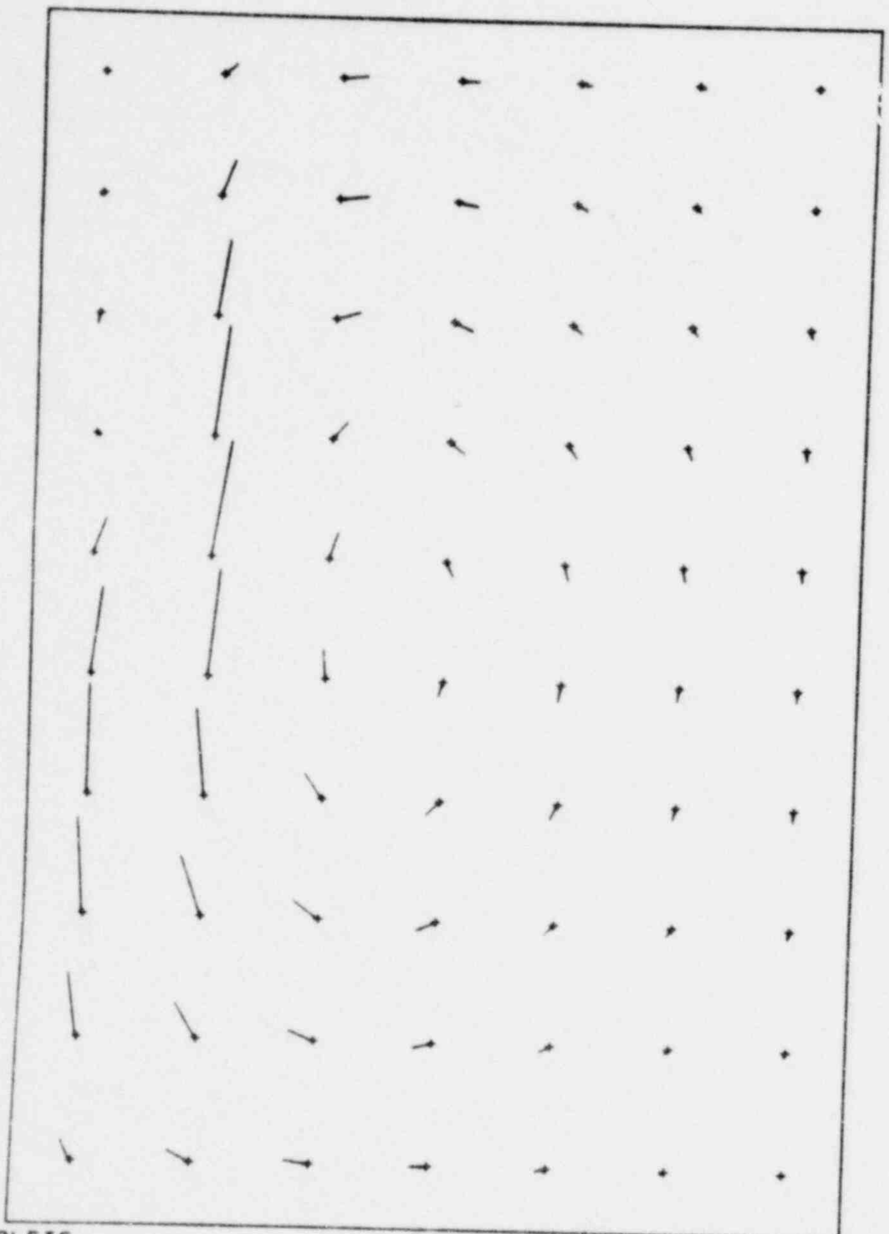

Fig. 4 Velocity vector plot for Sample Problem 1 illustrating how convection currents are produced in the liquid by the rising air bubble.

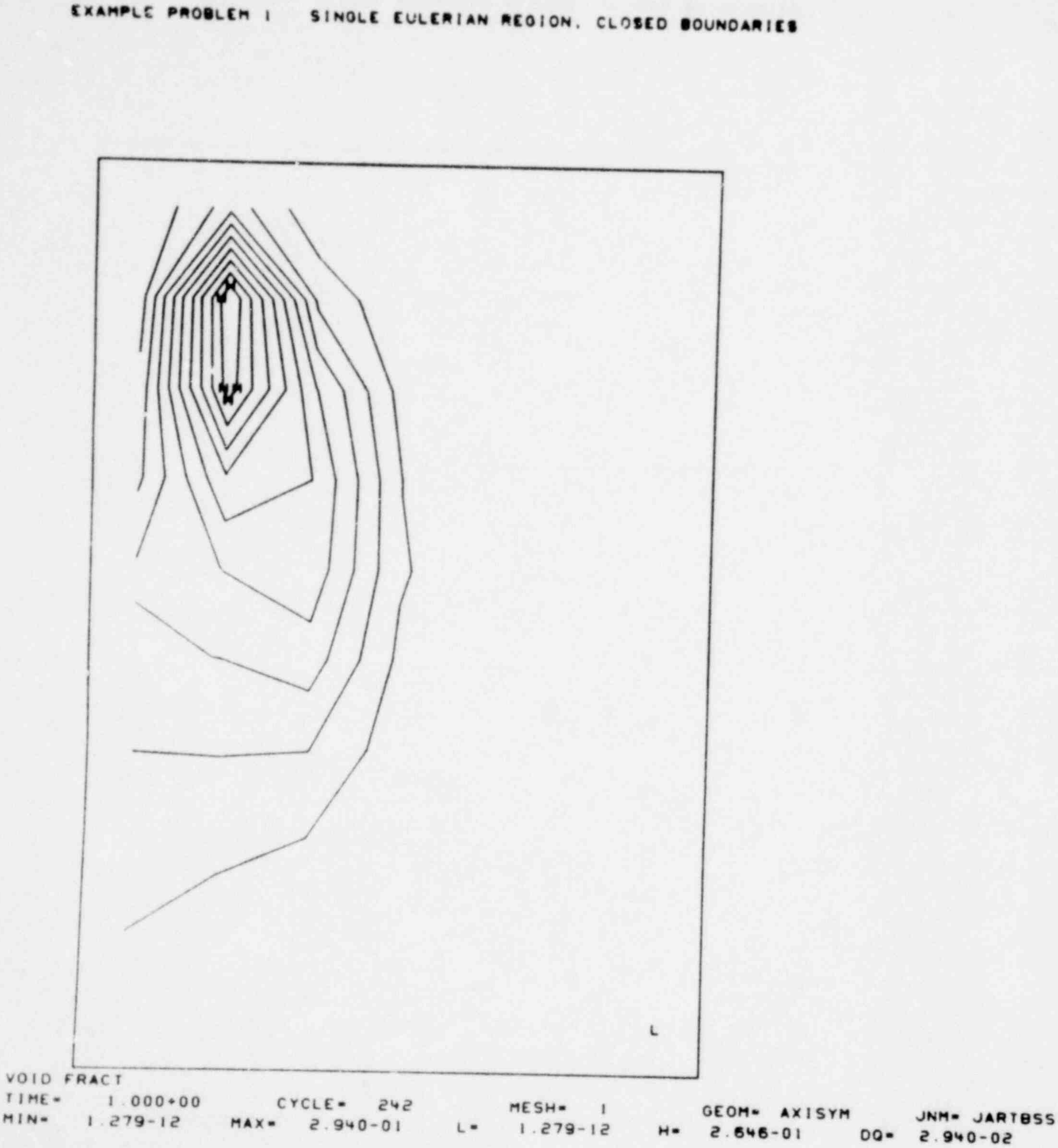

Fig. 5 Void fraction contour plot for Sample Problem 1 after the air bubble has risen to the top of the liquid.

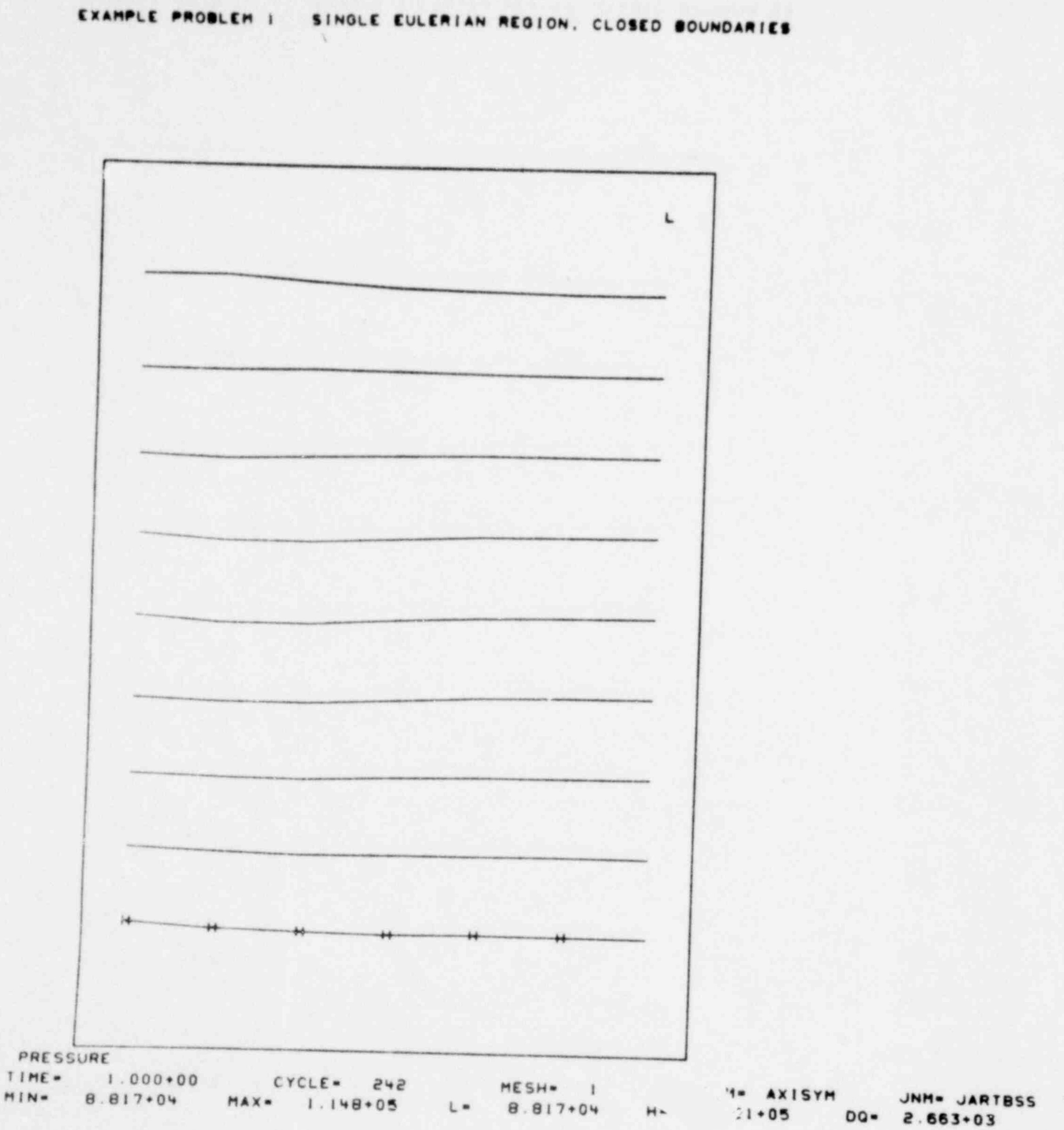

Fig. 6 Contour plot for Sample Problem 1 showing the calculated hydrostatic pressure gradient in the liquid.

2. SAMPLE PROBLEM 2: FLOW BOUNDARIES AND OBSTACLE CELLS

The configuration shown in Figure 7 demonstrates the use of specified flow boundaries and obstacle cells for a typical containment subcompartment analysis problem. The input data cards are shown in Figure 8. In this problem, compartments and passageways are formed by specifying regions of nonfluid, or obstacle cells (cards 11401 through 11403).

The fluid regions initially contain a vapor-liquid mixture at atmospheric pressure and a void fraction of 0.9. A vapor-liquid inflow of constant density and velocity is specified along the bottom boundary and a continuative outflow is specified along the right boundary of the mesh. The configuration is formed in Cartesian coordinates with gravitational force set to zero.

Velocity vector and pressure contour plots are shown in Figures 9 and 10 to illustrate the flow behavior at 0.5 seconds. The behavior is as expected: (1) Flow is diverted by the presence of obstacle boundaries, (2) Velocities are higher in the narrow constrictions, (3) Stagnant regions develop in corners and localized recirculation occurs in base regions, (4) Pressure buildup occurs in stagnating areas and gradients develop where velocities are generally rapidly changing.

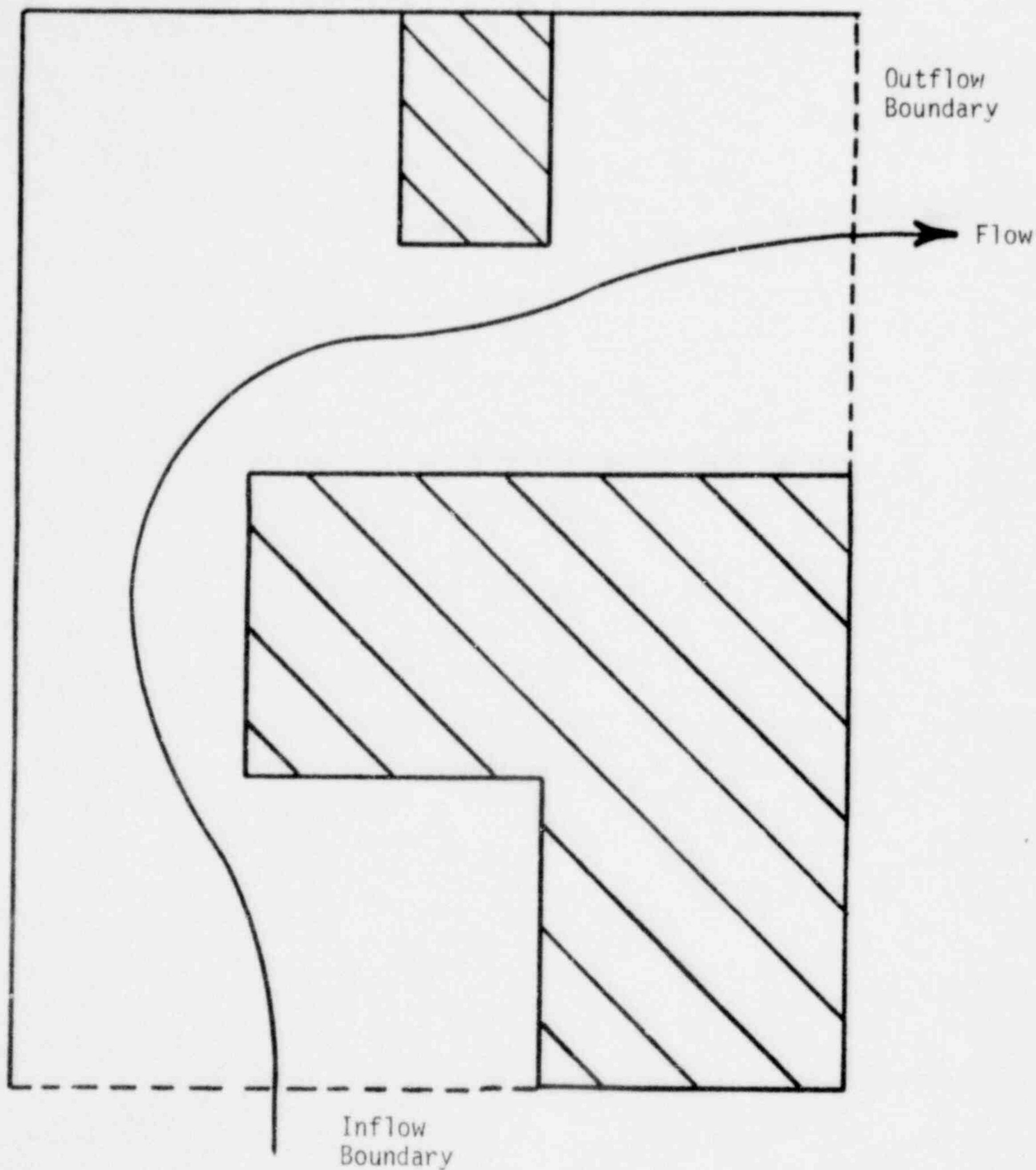

Fig. 7 Configuration for Sample Problem 2 a typical containment subcompartment problem, modeled with obstacle cells and inflow and outflow boundaries.

```
00100  'EXAMPLE PROBLEM 2: FLOW BOUNDARIES AND OBSTACLE CELLS'
***********BASIC PROBLEM INPUT
00110  0.0, 1.0, 0.001, SEC, 10.0, 20, XEQ
00120  0.001, 0.1, 0.0025, 2.0
00130  AUTODT, 1, 0.1, 1.0E06
00140  PRINT, NOPRINT, PRINT, NOPRINT, PRINT, 9999
00150    PLOTS, 0.9, 1 1 0 0 0 0 0 0 0 0 0 0
00200  1.5, 0.00010, 0.00010, 300, 5, 5
00210  0.0, FT SEC-2, 0.020, 0.38, BTU/HR-FT-DEGF, 10000.0
00220  1.5E-04, 2.8E-06, FT2/SEC, 1.0, 1.0, ATM, 23800.0, FT3, 1.0E04, 1
00230  0, 0.0, 0.0
00240  LASL, PT, LBF/IN2, DEGR, FT, SEC-1
***********EULERIAN REGION INPUT
11000  CARTSN, 11, 14, 1.0, 1.0, 1.0, FT, 0.0, 0.0
11010  NOSLIP, NOSLIP, NOSLIP, NOSLIP
11101  MIXTURE  2, 2, 8, 5, 0, 14.7, 600.0, 600.0, 0.9, 1.0
11102  MIXTURE  2, 6, 4, 9, 0, 14.7, 600.0, 600.0, 0.9, 1.0
11103  MIXTURE  2,10, 6,15, 0, 14.7, 600.0, 600.0, 0.9, 1.0
11104  MIXTURE  7,10, 8,12, 0, 14.7, 600.0, 600.0, 0.9, 1.0
11105  MIXTURE  9,10,12,15, 0, 14.7, 600.0, 600.0, 0.9, 1.0
***********OBSTACLE CELL INPUT
11401  NOSLIP, 9, 2, 12, 5
11402  NOSLIP  5, 6, 12, 9
11403  NOSLIP  7, 13, 8, 15
***********SPECIFIED BOUNDARY INPUT
11501  INFLOW  2, 1, 8, 1
11601  MIXTURE  14.7, 600.0, 600.0, 0.5, 1.0
11701  0.0, 10.0, 0.0, 10.0
11502  OUTFLOW  13, 10, 13, 15
.
```

Fig. 8 Input card listing for Sample Problem 2.

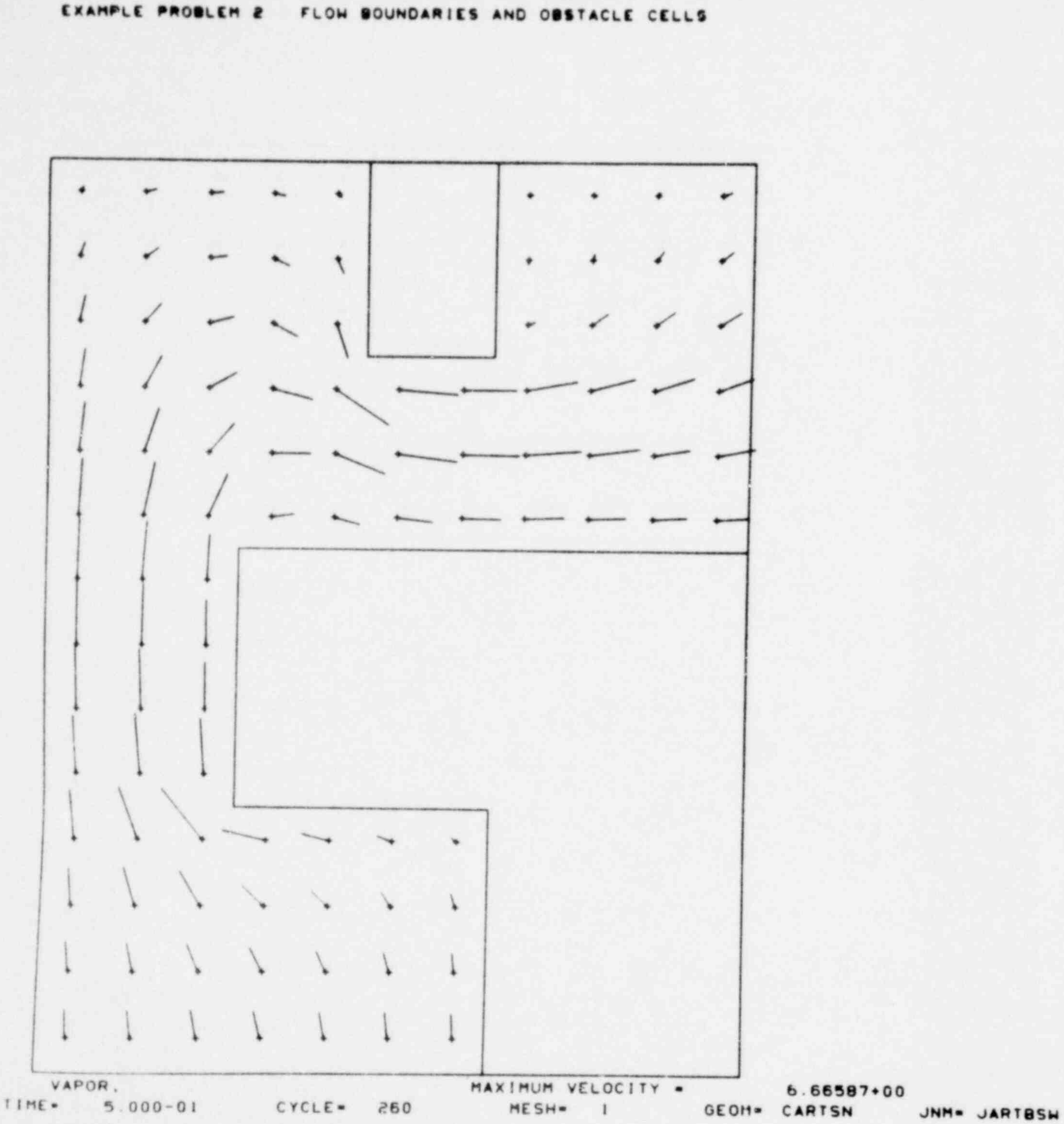

Fig. 9 Vapor velocity vector plot for Sample Problem 2 showing the flow diversion caused by the obstacles and the increase in velocities through the constricted areas.

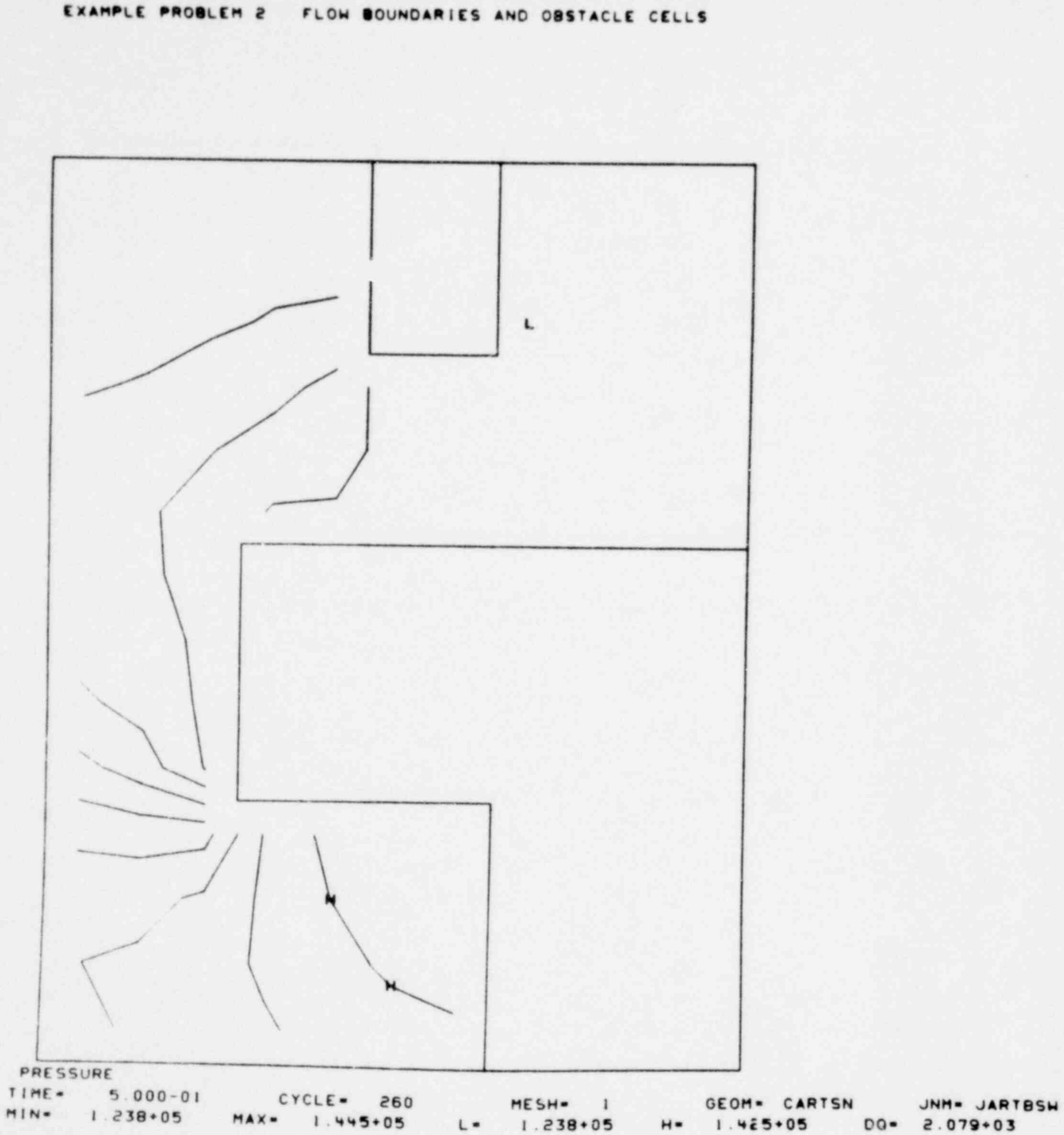

Fig. 10 Contour plot for Sample Problem 2 showing variations in the pressures resulting from velocity changes.

3. SAMPLE PROBLEM 3: MIXED DIMENSIONAL, MULTI-REGION COUPLING

Problem 3 demonstrates the Eulerian region coupling capability of BEACON. The configuration used in Sample Problem 2 was modeled by connecting several Eulerian regions as shown in Figure 11, thus eliminating the need for using obstacle regions. This problem was run to demonstrate that the results of modeling a containment with coupled Eulerian regions were consistent with the results obtained by modeling with a single region containing obstacle cells.

In addition to defining the fluid properties of the Eulerian regions, the connections between each region need to be defined. Input cards 006001 through 006004 in Figure 12 contain the information necessary to connect the five regions together.

The vapor velocity results for this problem are shown in Figure 13. As expected, these results match the results of Problem 2, showing the validity of the BEACON coupling logic.

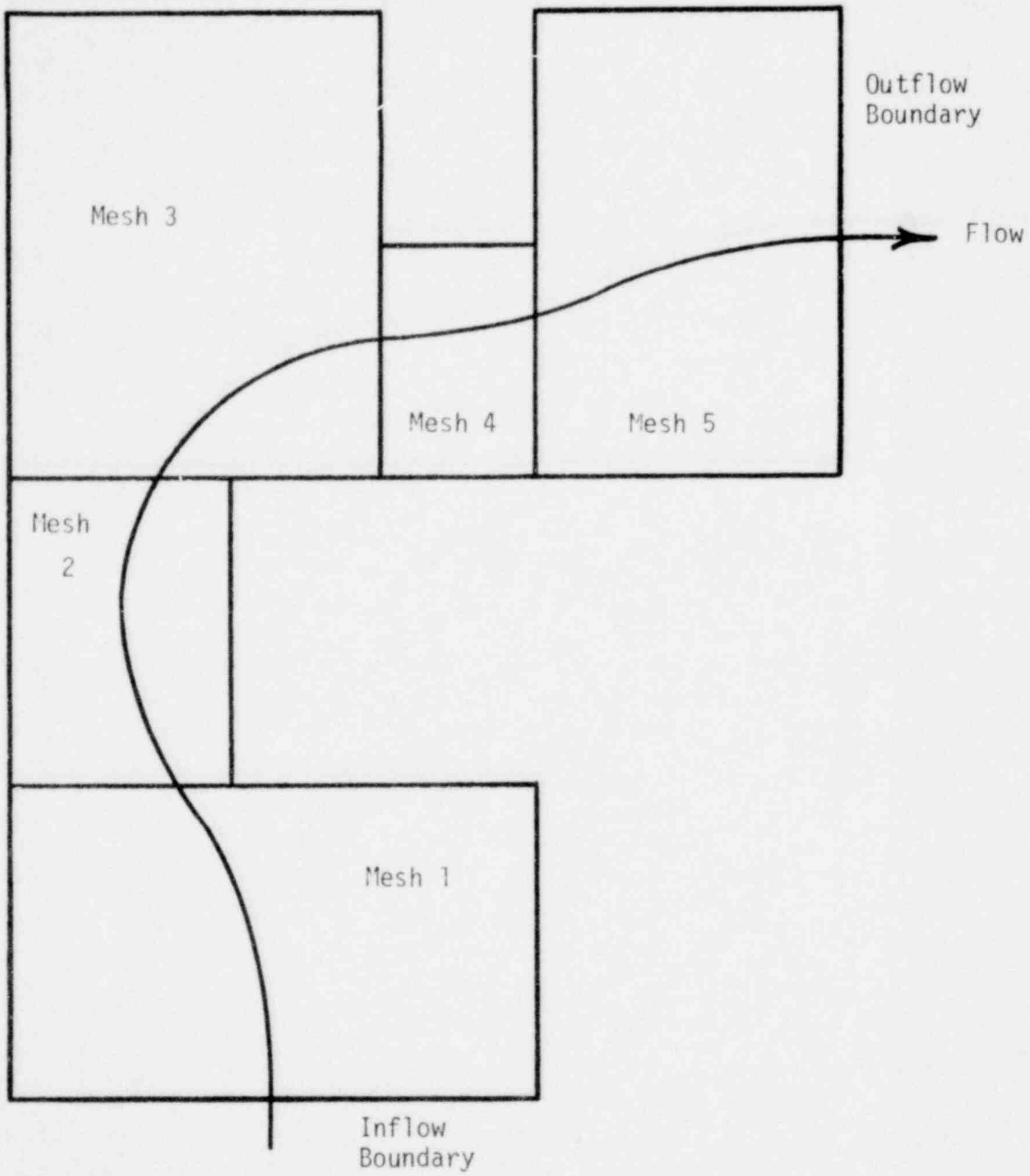

Fig. 11 Configuration for Sample Problem 3, a typical containment subcompartment problem, modeled by coupling a series of Eulerian regions.

```
00100  'EXAMPLE PROBLEM 3:  MIXED-DIMENSIONAL, MULTI-REGION COUPLING'
************BASIC PROBLEM INPUT
00110  0.0, 1.0, 0.001, SEC, 10.0, 20, XEQ
00120  0.001, 0.1, 0.0025, 2.0
00130  AUTODT, 1, 0.1, 1.0E06
00140  PRINT, NOPRINT, PRINT, NOPRINT, PRINT, 9999
00150    PLOTS, 0.45, 1 1 0 0 0 0 0 0 0 0 0 0
00160  MULTI, CONST, NOFLOSS
00170  5, 1, 1, 5
00200  1.5, 0.00010, 0.00010, 300, 5, 5
00210  0.0, FT SEC-2, 0.020, 0.38, BTU/HR-FT-DEGF, 10000.0
00220  1.5E-04, 2.8E-06, FT2/SEC, 1.0, 1.0, MM, 23800.0, FT3, 1.0E04, 1
00230  0, 0.0, 0.0
00240  LASL, PT, LBF/IN2,  EGR, FT, SEC-1
***********EULERIAN REGION INPUT
11000  CARTSN, 7, 4,   1.0, 1.0, 1.0, FT, 0.0, 1.0
21000  CARTSN, 3, 4,   1.0, 1.0, 1.0, FT, 0.0, 1.0
31000  CARTSN, 5, 6,   1.0, 1.0, 1.0, FT, 0.0, 1.0
41000  CARTSN, 2, 3,   1.0, 1.0, 1.0, FT, 0.0, 1.0
51000  CARTSN, 4, 6,   1.0, 1.0, 1.0, FT, 0.0, 1.0
11010  NOSLIP, NOSLIP, NOSLIP, NOSLIP
21010  NOSLIP, NOSLIP, NOSLIP, NOSLIP
31010  NOSLIP, NOSLIP, NOSLIP, NOSLIP
41010  NOSLIP, NOSLIP, NOSLIP, NOSLIP
51010  NOSLIP, NOSLIP, NOSLIP, NOSLIP
11101  MIXTURE  2, 2, 8, 5, 0, 14.7, 600.0, 600.0, 0.9, 1.0
21101  MIXTURE  2, 2, 4, 5, 0, 14.7, 600.0, 600.0, 0.9, 1.0
31101  MIXTURE  2, 2, 6, 7, 0, 14.7, 600.0, 600.0, 0.9, 1.0
41101  MIXTURE  2, 2, 3, 4, 0, 14.7, 600.0, 600.0, 0.9, 1.0
51101  MIXTURE  2, 2, 5, 7, 0, 14.7, 600.0, 600.0, 0.9, 1.0
***********SPECIFIED BOUNDARY INPUT
11501  INFLOW  2, 1, 8, 1
11601  MIXTURE  14.7, 600.0, 600.0, 0.5, 1.0
11701  0.0, 10.0, 0.0, 10.0
51501  OUTFLOW  6, 2, 6, 7
***********EULERIAN REGION COUPLING INPUT
006001  TOP  1, 2, 5, 3, 2, 2, 2, 3
006002  TOP  2, 2, 5, 3, 3, 2, 2, 3
006003  RIGHT  3, 6, 2, 3, 4, 2, 2, 3
006004  RIGHT  4, 3, 2, 3, 5, 2, 2, 3
*
```

Fig. 12 Input card listing for Sample Problem 3.

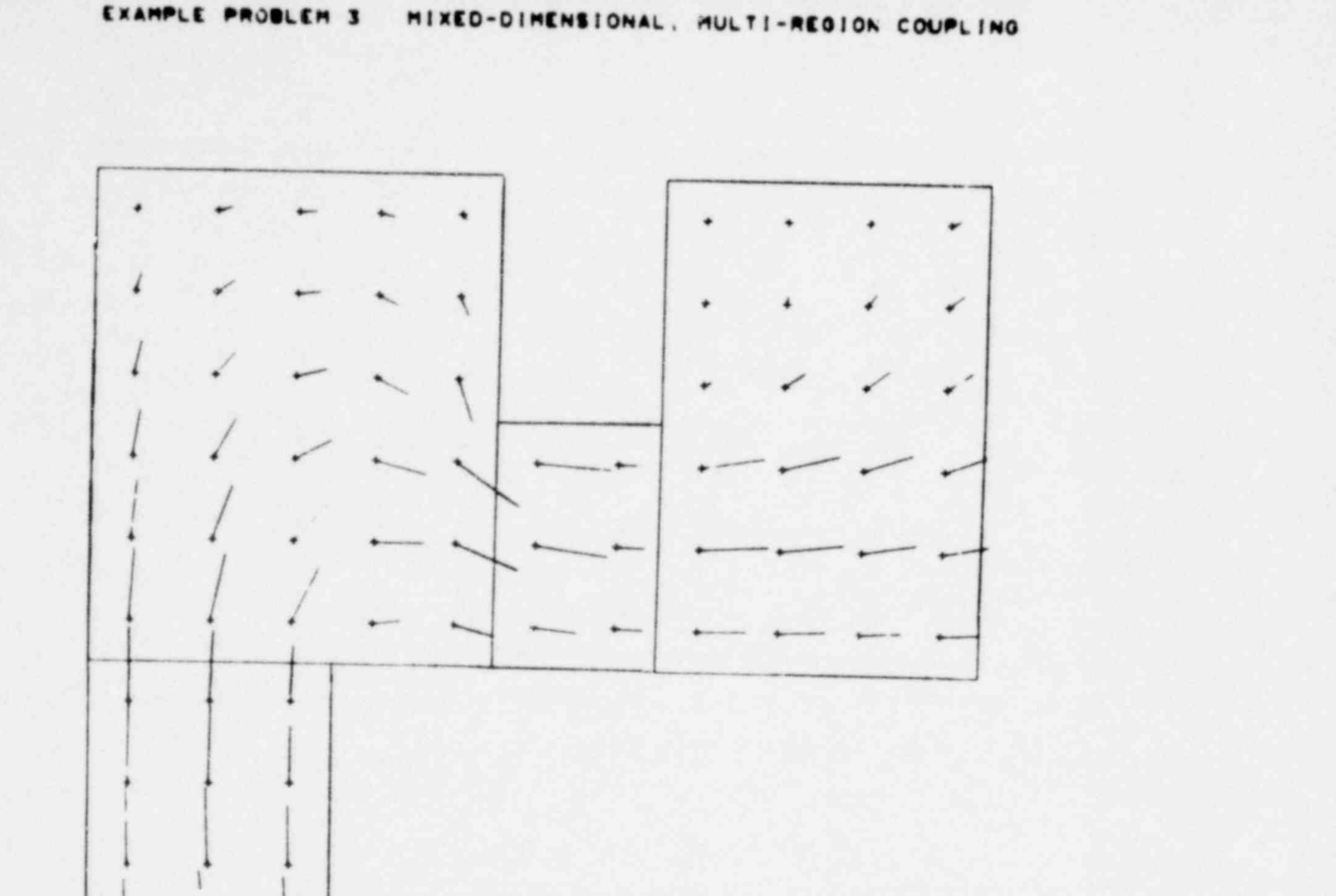

Fig. 13 The vapor velocity vector plot for Sample Problem 3, modeled with a series of coupled Eulerian regions, shows results that are consistent with those of Sample Problem 2, a single region modeled with obstacle cells.

4. SAMPLE PROBLEM 4: LUMPED PARAMETER AND UNEQUAL AREA COUPLING

The configuration shown in Figure 14 demonstrates lumped parameter modeling and other aspects of the BEACON mixed-dimensional, multi-region coupling capability.

The configuration is a steady-state flow problem in which pressure differences between the two semi-infinite lumped parameter volumes establish a flow from left to right, with flow accelerating and then decelerating in the 1-D regions. The two one-dimensional regions have different cross-sectional flow areas with a ratio of one to two. Figure 15 shows the required input data. Whenever unequal flow area coupling is desired, card 00160 must so indicate. The change in flow area is obtained with the appropriate input of cell dimensions on cards 11000 and 21000. The lumped parameter regions are used in this particular case to model invariant flow boundaries. The flow is two-phase with a void fraction of 0.9. No interphasic mass transfer is assumed.

The pressure and velocity variation in the 1-D regions at steady-state conditions are shown in Figure 16. The variation is as expected and typical of the behavior expected from 1D pipe flow analysis. The pressure rapidly decreases as flow velocity increases in the first 1-D region, and actually drops below the pressure of the receiving lumped parameter region due to the acceleration of the fluid. Then, in the second and larger 1-D region the flow starts to decelerate due to the change in flow area and continuity considerations. There is also a corresponding change in the pressure gradient.

This problem also demonstrates the separated flow, unequal velocity capability of BEACON. Initially, the liquid flow lags the vapor flow due to inertial differences and to a nonhomogeneous, interphasic momentum exchange function modeling. At the abrupt area change the vapor undergoes a rapid deceleration and approaches a discontinuity at the sudden expansion. However, the inertia of the liquid resists the sudden velocity change, with the result being a less rapid decceleration of the liquid flow and liquid velocities higher than the vapor velocities in the larger 1-D region.

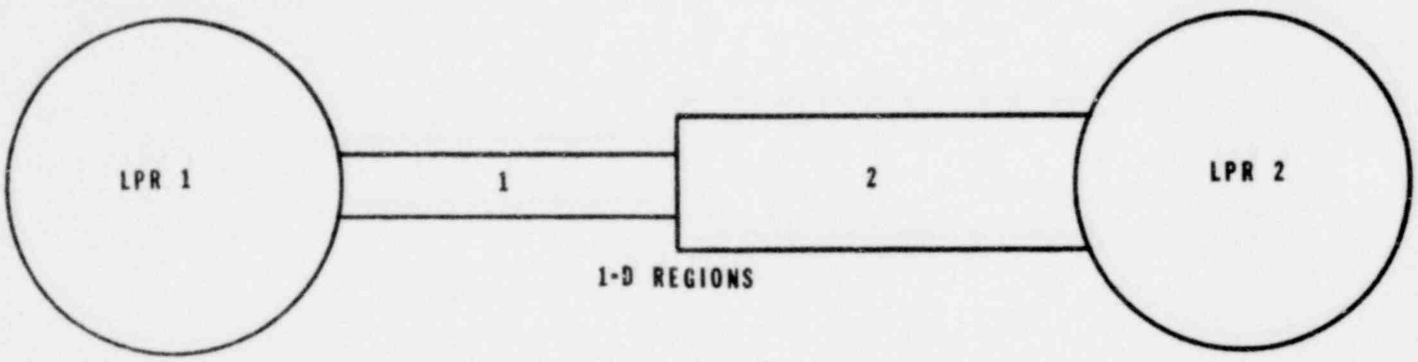

Fig. 14 Configuration for Sample Problem 4, a mixed-dimensional, multi-region problem with unequal flow area coupling and separated flow between two lumped parameter regions.

```
00100   'EXAMPLE PROBLEM 4:  LUMPED PARAMETER AND UNEQUAL AREA COUPLING'
***********BASIC PROBLEM INPUT
00110   0.0, 1.0, 0.0010, SEC, 2.0, 20, XEQ
00120   0.0010, 0.02, 0.0020, 0.1, 0.0025, 5.0
00130   AUTODT, 10, 0.1, 10.0
00140     PRINT, NOPRINT,    PRINT,    PRINT,    PRINT, 9999
00150   NOPLOTS, 0.45, 0 0 0 0 0 0 0 0 0 0 0 0
00160   MULTI, UNEQUAL, NOFLOSS
00170   2, 1, 1, 2
00180   2, 0.01
00200   1.5, 0.00010, 0.00010, 300, 5, 5
00210   -32.174, FT SEC-2, 0.020, 0.38, BTU/HR-FT-DEGF, 10000.0
00220   4.0E-06, 2.0E-06, FT2/SEC, 1.0, 1.0, MM, 500000.0, FT3, 1.0E20, 3
00230   0, 0.0, 0.0
00240   LASL, PT, LBF/IN2, DEGR, FT, SEC-1
***********EULERIAN REGION INPUT
11000   CARTSN  5, 1, 1.0, 0.5, 3.28084, FT, 0.0, 0.0
21000   CARTSN  5, 1, 1.0, 1.0, 3.28084, FT, 0.0, 0.0
11010   NOSLIP, NOSLIP, NOSLIP, NOSLIP
21010   NOSLIP, NOSLIP, NOSLIP, NOSLIP
11101   MIXTURE  2, 2, 6, 2, 0, 20.0, 700.0, 700.0, 0.9, 1.0
21101   MIXTURE  2, 2, 6, 2, 0, 20.0, 700.0, 700.0, 0.9, 1.0
***********LUMPED PARAMETER REGION INPUT
12000   ZEROD  1.0E20, FT3, 10000.0, 0.0, 0.0
12010   MIXTURE  30.0, 700.0, 700.0, 0.9, 1.0
22000   ZEROD  1.0E20, FT3, 10000.0, 0.0, 0.0
22010   MIXTURE  20.0, 700.0, 700.0, 0.9, 1.0
***********EULERIAN REGION COUPLING INPUT
06001   RIGHT  1, 6, 2, 1, 2, 2, 2, 1
***********LUMPED PARAMETER COUPLING INPUT
07001   LEFT  1, 2, 2, 1, 1.0
07002   RIGHT  2, 6, 2, 2, 1.0
*
```

Fig. 15 Input card listing for Sample Problem 4.

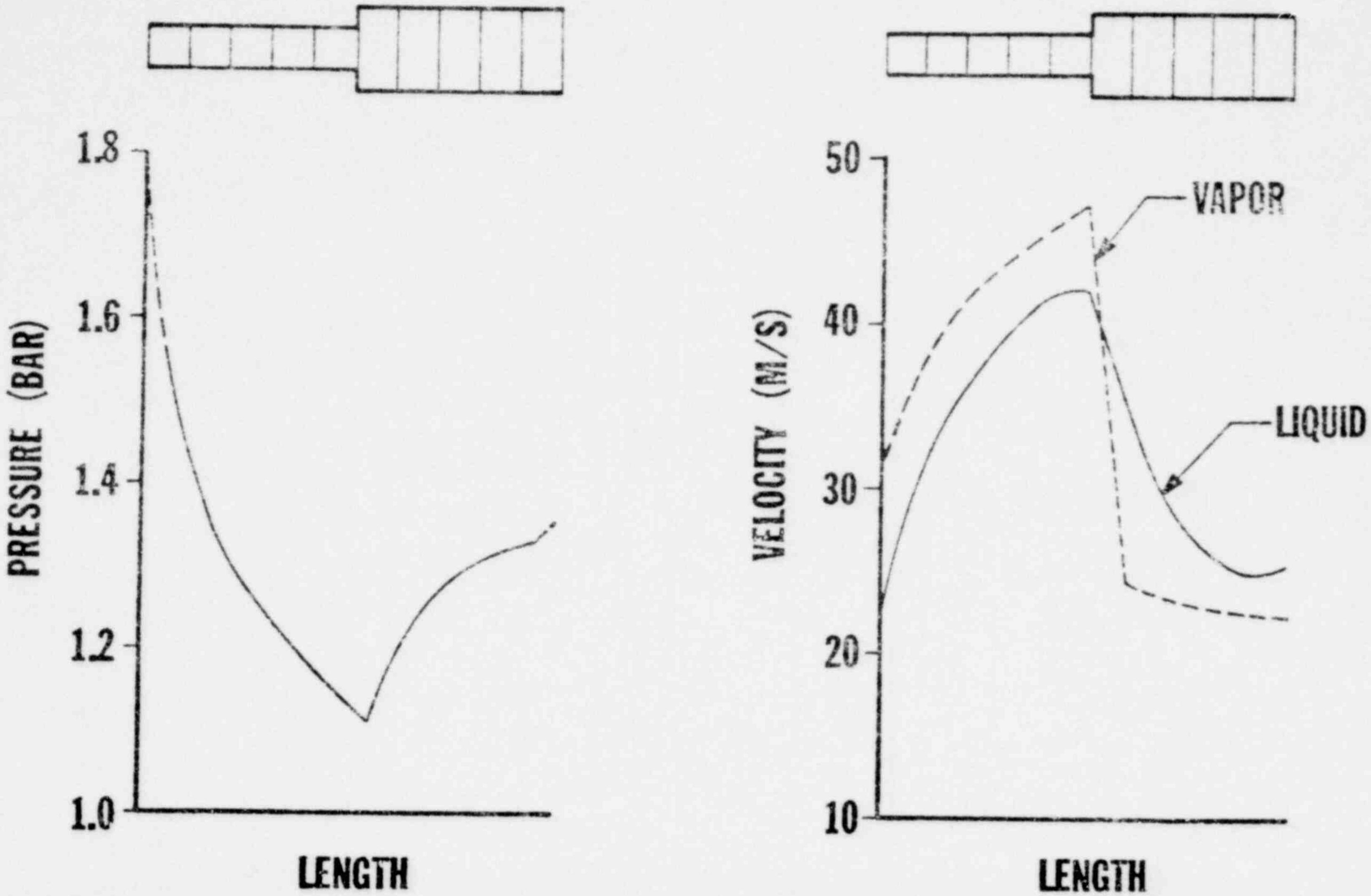

Fig. 16 Pressure and velocity variation in coupled one-dimensional regions showing pressure decrease due to flow velocities and corresponding separated flow effects.

5. SAMPLE PROBLEM 5: SOURCE CELL ADDITION

Source cell modeling is demonstrated with this sample problem. A two-compartment arrangement is configured is shown in Figure 17. Four source cells are located in the lower and smaller compartment to introduce a vapor mass at an appropriate enthalpy. This problem demonstrates how a steam pipe break in a hypothetical loss-of-coolant accident could be modeled. The mesh compartments initially contain a vapor-liquid mixture of void fraction 0.5. Interphasic mass transfer is assumed to be zero. The mesh and obstacle walls are assumed rigid with no-slip boundary conditions.

Input data for this problem are shown in Figure 18. The source input cards are the 3000 numbered series. For each source, the mass flow rate is initially zero, increasing to 100 kg/sec at 0.01 seconds and remaining constant for the duration of the problem. The enthapy level remains constant throughout, and must be input even if the mass flow rate is zero.

Plot output results are shown for a problem time of 1.0 seconds. The vapor velocity vector plot in Figure 19 shows that velocities in the constriction and in the lower compartment are still high but that in the upper compartment flow conditions are starting to stagnate due to the lack of any place for the flow to go. The void fraction contours in Figure 20 indicate that the vapor source has essentially displaced the initial vapor-liquid mixture in the lower compartment. Lastly, the pressure distribution shown in Figure 21 is as expected, with the location of highest pressure being furthest from the constriction and in an area of stagnation.

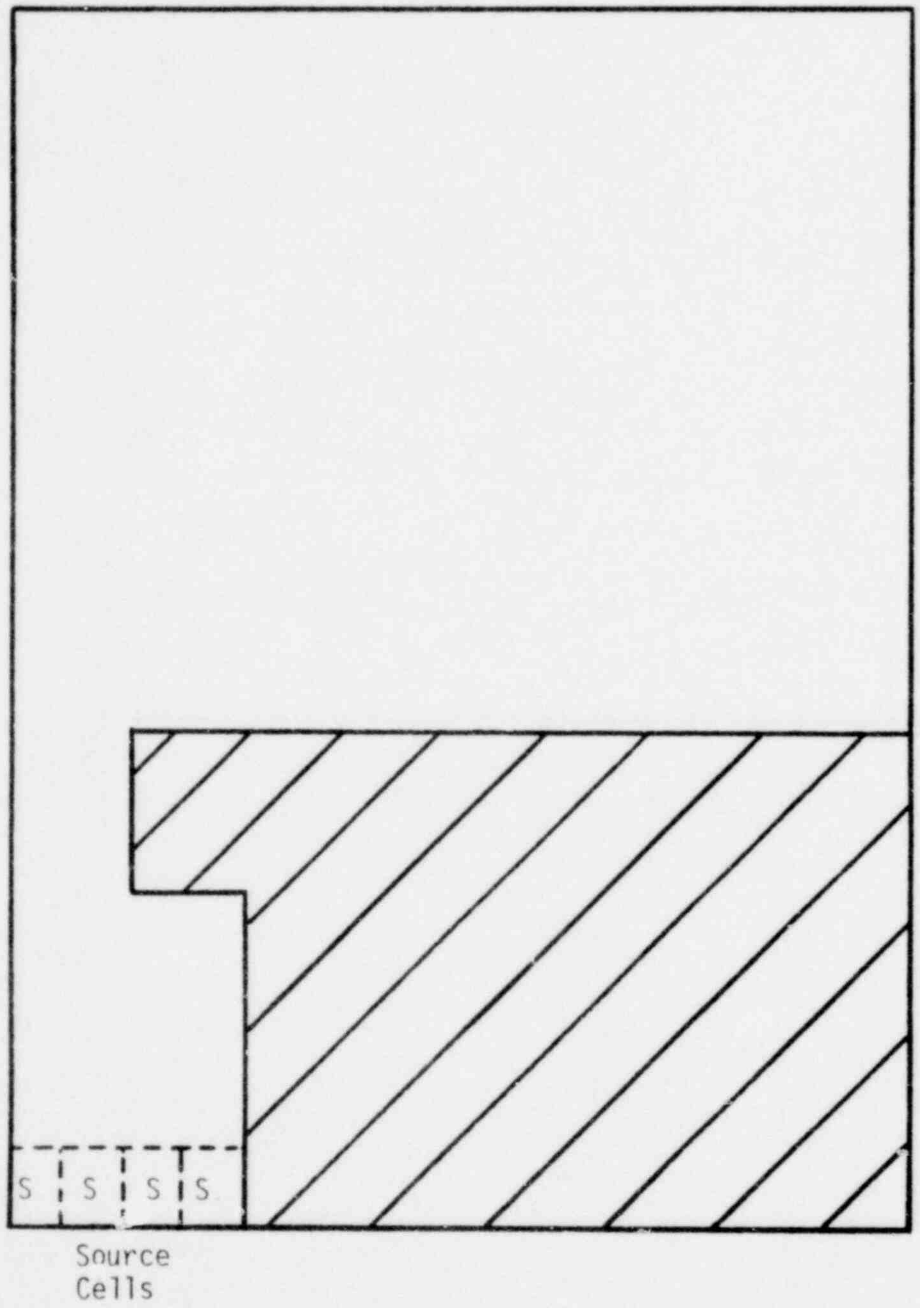

Fig. 17 Configuration for Sample Problem 5 demonstrating the use of source cells to introduce a steam flow into a two-compartment containment.

```
00100  'EXAMPLE PROBLEM 5:  SOURCE CELL ADDITION'
************BASIC PROBLEM INPUT
00110  0.0, 1.00,  0.0005, SEC, 2.0, 20, XEQ
00120  0.0005, 0.020, 0.001, 0.1, 0.005, 3.0
00130  AUTODT, 10, 0.1, 10.0
00140  PRINT, NOPRINT, PRINT, PRINT, PRINT, 9999
00150    PLOTS, 0.9, 1 1 0 0 0 0 0 0 0 0 0
00200  1.5, 0.0001, 0.0001, 100, 5, 5
00210  0.0,       FT SEC-2, 0.020, 0.38, BTU/HR-FT-DEGF, 20000.0
00220  4.0E-06, 2.0E-06, FT2/SEC, 1.0, 1.0, MM, 119000.0, FT3, 1.0E20, 3
00230  0, 0.0, 0.0
00240  LASL  PT  LBF/IN2  DEGR  FT  SEC-1
************EULERIAN REGION INPUT
11000  CARTSN, 15, 15, 1.5, 2.0, 1.0, M, 0.0, 0.0
11010  NOSLIP, NOSLIP, NOSLIP, NOSLIP
11101  MIXTURE  2, 2, 5, 5, 0, 25.0, 700.0, 700.0, 0.5, 0.0
11102  MIXTURE  2, 6, 3, 7, 0, 25.0, 700.0, 700.0, 0.5, 0.0
11103  MIXTURE  2, 8,16,16, 0, 25.0, 700.0, 700.0, 0.5, 0.0
************OBSTACLE CELL INPUT
11401  NOSLIP  6, 2, 16, 5
11402  NOSLIP  4, 6, 16, 7
************SOURCE INPUT
003010  STEAM  1, 2, 2, 3011, 0.0, DEG, 1.0, 1.0, 1.0, 0.0
003060  STEAM  1, 3, 2, 3011, 0.0, DEG, 1.0, 1.0, 1.0, 0.0
003110  STEAM  1, 4, 2, 3011, 0.0, DEG, 1.0, 1.0, 1.0, 0.0
003160  STEAM  1, 5, 2, 3011, 0.0, DEG, 1.0, 1.0, 1.0, 0.0
003011  SEC, KG/SEC, J/KG, FT SEC-1
003012  0.0, 0.0,              2.8E06, 0.0
003013  0.01, 100.0,           2.8E06, 0.0
003014  3.00, 100.0,           2.8E06, 0.0
.
```

Fig. 18 Input card listing for Sample Problem 5.

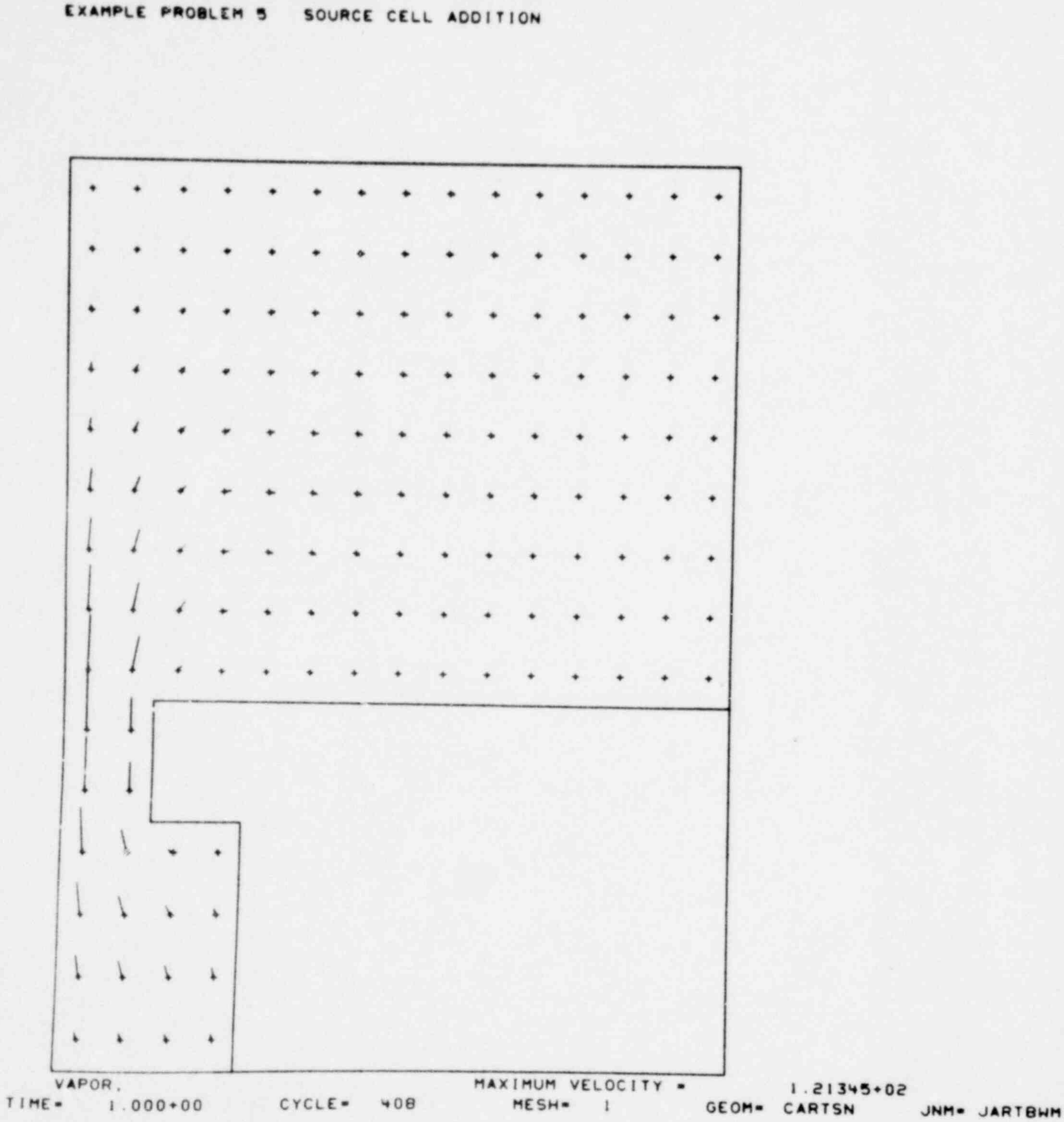

Fig. 19 Vapor velocities for Sample Problem 5 increase in the constricted area and stagnate in the large upper compartment.

Fig. 20 Void fraction contour plot for Sample Problem 5 illustrating the displacement of the initial vapor-liquid mixture from the lower compartment by the steam.

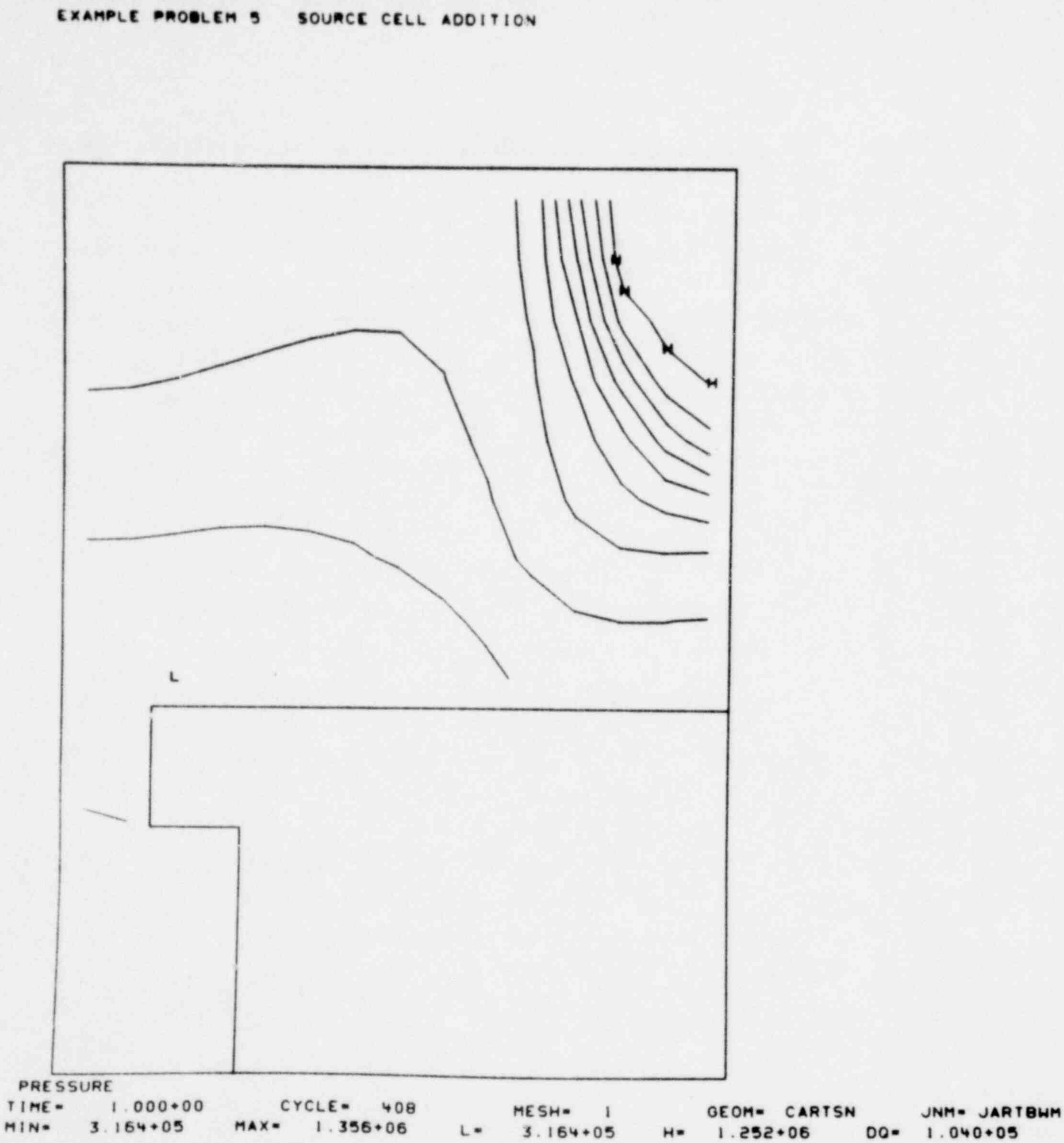

Fig. 21 Pressure contour plot for Sample Problem 5 showing pressurization of the upper compartment because of stagnation effects.

6. SAMPLE PROBLEM 6: PARTIAL FLOW CELLS

This problem demonstrates the new partial flow capability of BEACON/MOD2A. This capability is used to model obstacles that are smaller in size (volume) than the computational fluid cells. In a partial flow cell or region, the volume and flow areas are reduced from their normal unrestricted values. Unlike an obstacle cell which has complete flow blockage, a partial flow cell still allows fluid to pass through but at a reduced level. The remaining fluid is diverted to the surrounding fluid cells subsequently changing the flow pattern in the vicinity of the partial flow cell. This allows for a coarser nodalization, and, at the same time, factors in the gross effects of obstructions to the flow.

In this problem configuration (Figure 22), partial flow barriers are alternately placed, forcing the flow to travel in a labyrinthine path. The regions of partial flow cells are specified by cards 11301 through 11303 of Figure 23. The flow areas and volumes of these regions are reduced to 0.1 of the normal unrestricted cell values. A flow resistance coefficient of 3.0 is specified for both the radial and axial directions. The top and bottom boundaries of the mesh are continuative outflow and inflow boundaries, respectively.

The effects of the partial flow regions on the flow can be seen by the fluid velocity vector and pressure gradient patterns shown in Figures 24 and 25, respectively. The flow is partially diverted as it approaches the restricted cells. The velocities increase and the pressure gradients steepen as the flow progresses through the reduced areas.

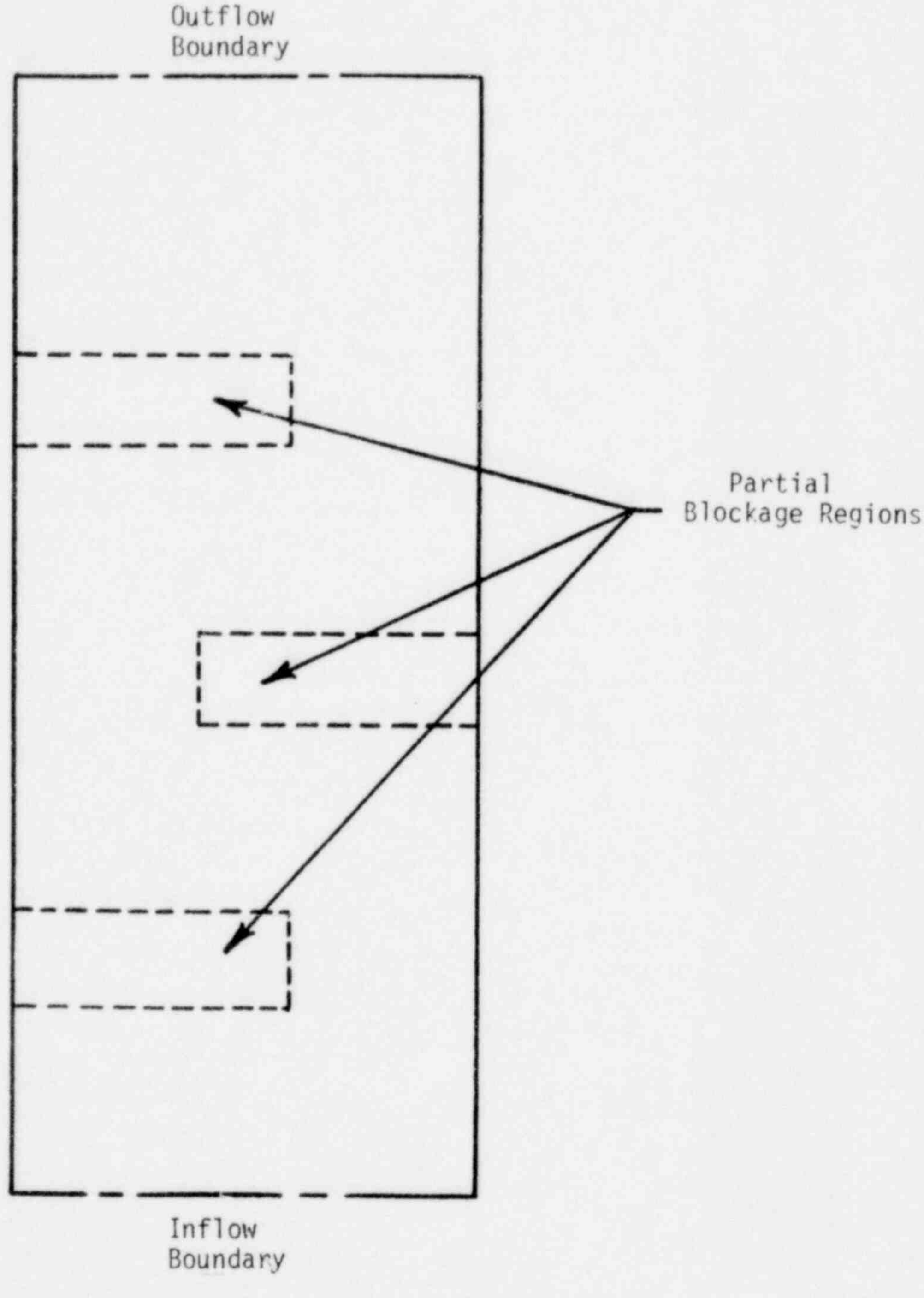

Fig. 22 Configuration for Sample Problem 6 showing locations of the partial flow blockages.

```
00100   *EXAMPLE PROBLEM 6:  PARTIAL FLOW TEST CASE
00110   0.0, 0.5, 0.0001, SEC, 2.0, 1, XFC
00120   0.050,  2.0
00130   AUTODT, 0, 0.1, 1.5
00140   PRINT, NOPRINT, PRINT, NOPRINT, NOPRINT, 9999
00150     PLOTS, 0.9, 1 1 0 0 0 0 0 0 0 0 0 0 0
00200   1.5, 0.00010, 0.00010, 300, 5, 0
00210   0.0, FT SEC-2, 0.020, 0.38, BTU/HR-FT-DEGF, 1.0E06
00220   0.0, 0.0, FT2/SEC, 1.0, 1.0, MM, 23800.0, FT3, 1.0E04, 1
00230   0, 0.0, 0.0
00240   LASL, PT, N/M2, DEGK, M, SEC-1
11000   CARTSN,  5, 12, 4.0, 4.0, 2.6667, FT, 0.0, 1.0
11101   MIXTURE  2, 2, 6,13, 0, 1.0E05, 309.1, 309.1, 0.999, 0.9
11501   INFLOW  2, 1, 5, 1
11601   MIXTURE  2.0E05, 309.1, 309.1, 0.999, 0.9
11701   0.0, 20.0, 0.0, 20.0
11502   OUTFLOW  2, 14, 6, 14
11301   2, 4, 4, 4, 0.1, 3.0, 3.0
11302   4, 7, 6, 7, 0.1, 3.0, 3.0
11303   2,10, 4,10, 0.1, 3.0, 3.0
.
```

Fig. 23 Input card listing for Sample Problem 6.

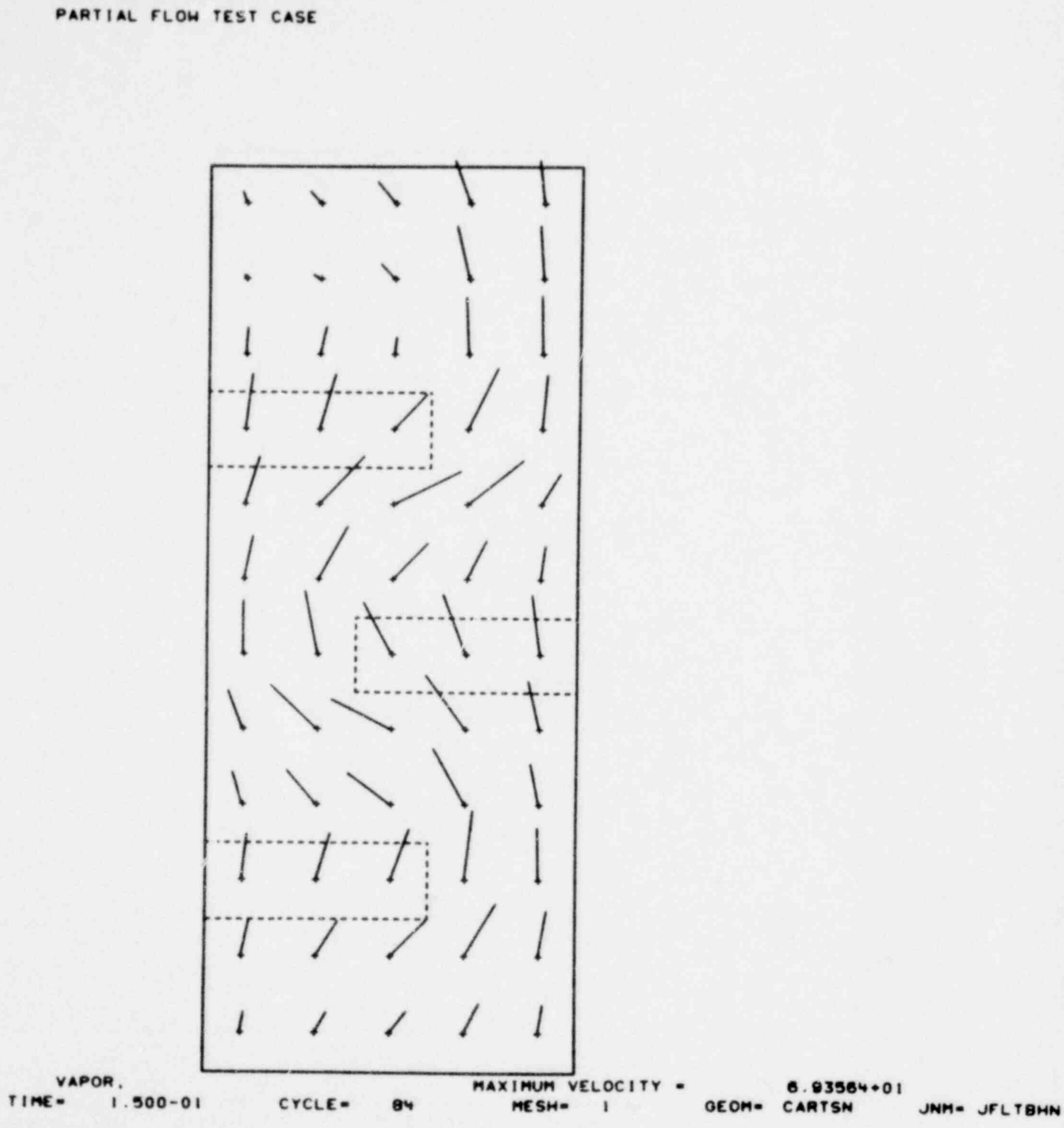

Fig. 24 Vapor velocity vector plot for Sample Problem 6 showing partial, but not complete, diversion of the flow due to partial flow restrictions in its path.

PARTIAL FLOW TEST CASE

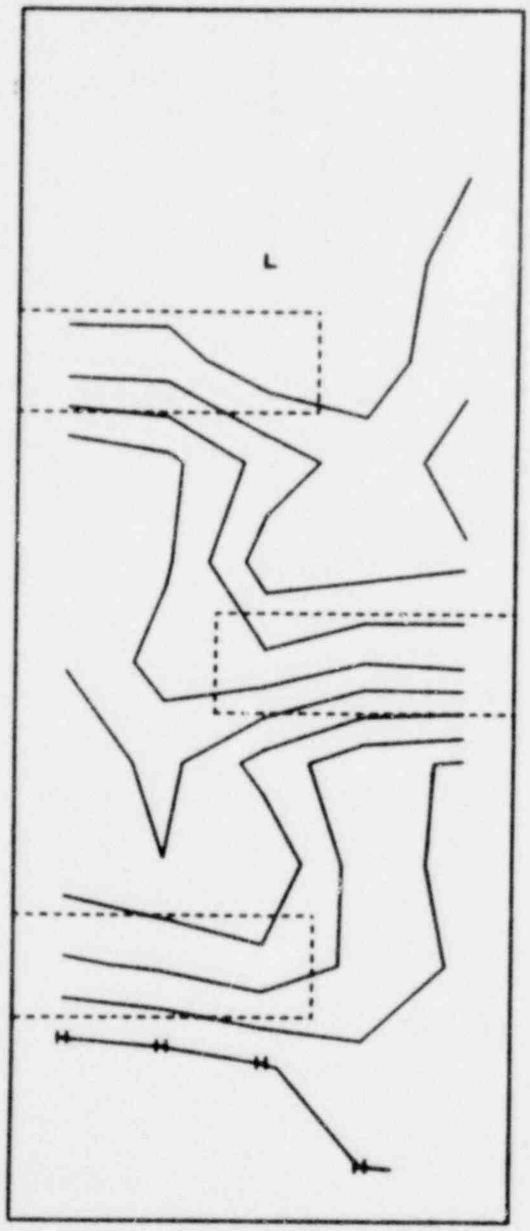

Fig. 25 Pressure contour plot for Sample Problem 6 showing steepened gradient through the partial flow cells.

7. SAMPLE PROBLEM 7: DRY, MULTI-COMPARTMENT CONTAINMENT WITH WALL FILM AND HEAT STRUCTURES

Sample problem 7 demonstrates three new modeling capabilities of BEACON/MOD2A:

(1) Wall film modeling

(2) Heat structure modeling

(3) Variable mesh spacing.

The problem configuration in Figure 26, represents a typical dry containment subcompartment arrangement. The room designations, physical dimensions, and flow conditions were taken from a previous Battelle-Frankfurt experiment. However, since this problem was set up only for code checkout purposes, the results are not intended to be compared with test data. The rooms are connected by short flow nozzles. A steam break is assumed to occur in the far corner of Room 6.

This problem is modeled in Cartesian coordinates and the nodalization is shown in Figure 27. Rooms 6 and 4 are modeled by two-dimensional regions (meshes 1 and 3, respectively). Room 9 is much larger in volume than rooms 6 and 4 and therefore is modeled as a lumped parameter region. The room connections are modeled by one-cell, one-dimensional meshes.

There are a large number of heat structures for this problem. Each material present in a room is represented by one heat structure as shown in Figure 28. Heat structures connected to lumped parameter regions are not spatially oriented.

Input for variable mesh spacing are specified by cards 11020 and 31030 of Figure 29. Film modeling is specified only for the two-dimensional regions (cards 11050 and 31050). Card 250 specifies film modeling parameters.

Three variations of this problem were run to illustrate the effects of wall film and heat structures:

(1) Configuration without heat structures and without wall film modeling (applicable input of Figure 29 deleted),

(2) Configuration with heat structures but without wall film modeling (applicable input deleted).

(3) Configuration with heat structures and with wall film modeling. The film in one-dimensional regions, being of only minor consequence, was turned off for computational efficiency. Also, film modeling in a lumped parameter region is not allowed.

Each of these variations were executed to a problem time of 0.5 s. The effect of these variations on room pressure and temperature are compared in Figures 30 and 31. The results are as expected. Without heat structures and film modeling, the configuration is adiabatic and pressures and temperatures are expected to be highest. With the presence of heat structures, dropwise steam condensation occurs and heat is transferred to the walls causing pressures and temperatures to be lower. The formation of a liquid film on the walls, however, decreases the effective heat transfer to the walls. Therefore, the values are higher than those without film. Observation of Figure 30 shows that the rate at which the pressure rises in Room 6 is higher than that in Room 4 for the first 0.2 s. Beyond this time, the pressure curves in the two rooms start to converge as the fluid starts to accumulate in Room 4. Based on this pressure difference in the two rooms, the fluid velocity in Mesh 2 is observed to increase until it reaches a maximum value at 0.2 s, beyond which it monotonically decreases with time. A similar velocity peak, observed in Mesh 4, occurs later at 0.3 s, since the rate of pressure increase in Room 9 is much smaller due to its relatively large volume. Also, because of relatively small pressure in Room 9, the magnitude of maximum velocity observed in Mesh 4 is about 50% larger than the maximum velocity in Mesh 2 (381 m/s compared to 247 m/s).

Selected velocity vector and contour plots are shown in Figures 32 through 37 to illustrate the spatial dependence of these variables at a given time. Figure 32 shows the gas phase velocities at 0.08 s. Velocities in Room 9, which is modeled as a lumped parameter region, are assumed zero. Hence Room 9 is not included in Figure 32. The velocities in Room 6 are generally higher than those in Room 4 as expected during an early part of the transient due to larger pressure differential between Rooms 6 and 4 as compared to that between Rooms 4 and 9. The velocity vectors in the top right corner of Room 6 are at 45° angle due to a combined effect of the discharge from the source and a positive pressure gradient from left to right. Figures 33 and 34 show constant pressure and vapor temperature lines in Room 6 at 0.08 s. The maximum pressure and temperature are observed near the source, as expected. Figure 35 shows the contours of film mass. Since saturated steam was discharged by the source, highest film mass is observed near the source location due to large condensation rates. Also, the gravity tends to accumulate the liquid on the floor directly under the source. Spatial dependence of film velocities is presented in Figure 36 for all the meshes during the later part of the transient (0.5 s). Since, film is not allowed in a lumped parameter region, Room 9 has not been shown in Figure 36. The film velocities are observed to be highest near the nozzles due to large fluid velocities. Since at this time, the fluid velocities are higher in Room 4 as compared to Room 6, as discussed earlier, higher film velocities are observed in Room 4. The large film velocity indicated at the bottom of Room 4 is physically unrealistic, and arises as a result of crude nodalization in which the large ambient fluid velocity is used for this film velocity calculation. Careful nodalization is required to properly represent certain configurations. Further study is required to establish general guidelines for nodalization. Finally, Figure 37 shows constant film temperature lines for Room 6 at 0.5 s. The highest temperature is observed near the source, as expected.

Comparisons of CPU time required to run each of the three cases were also made. With no flim or heat structures the CPU time was 259 seconds, with heat structures only it was 283 seconds, and with both film and heat structures it was 385 seconds.

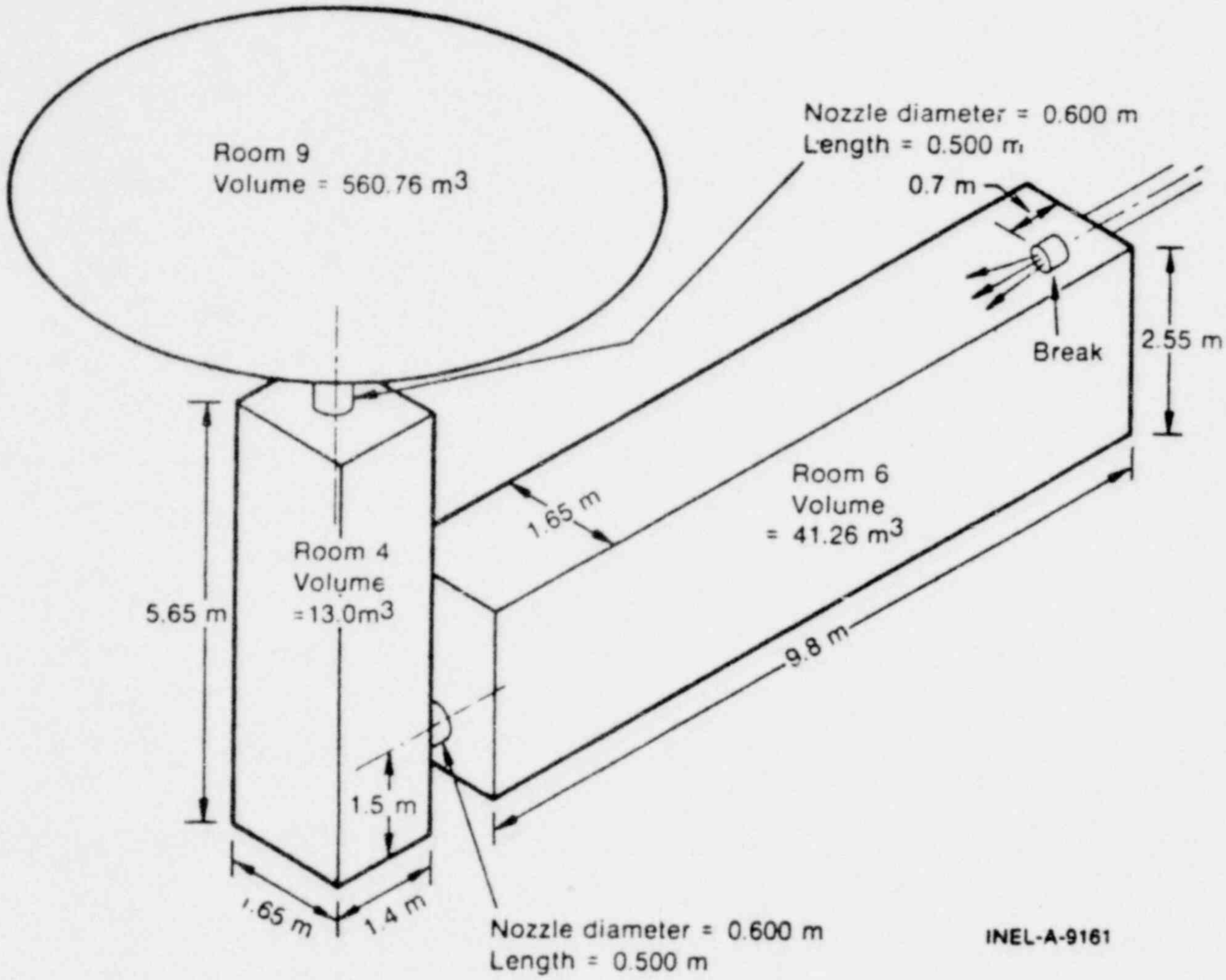

Fig. 26 Configuration for Sample Problem 7 which simulates a primary coolant pipe break into the first in a series of interconnected rooms.

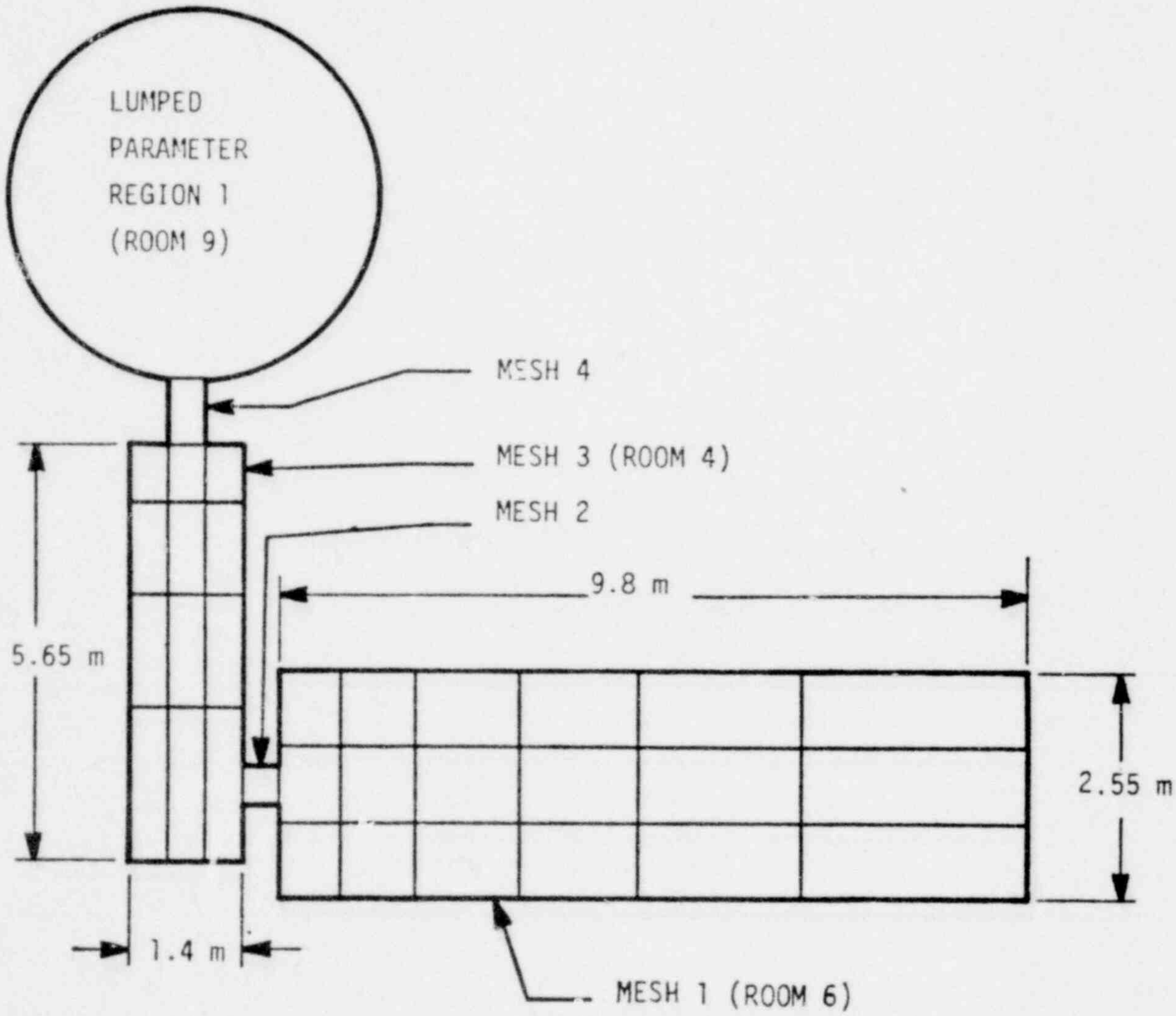

Fig. 27 Variable mesh nodalization for Sample Problem 7.

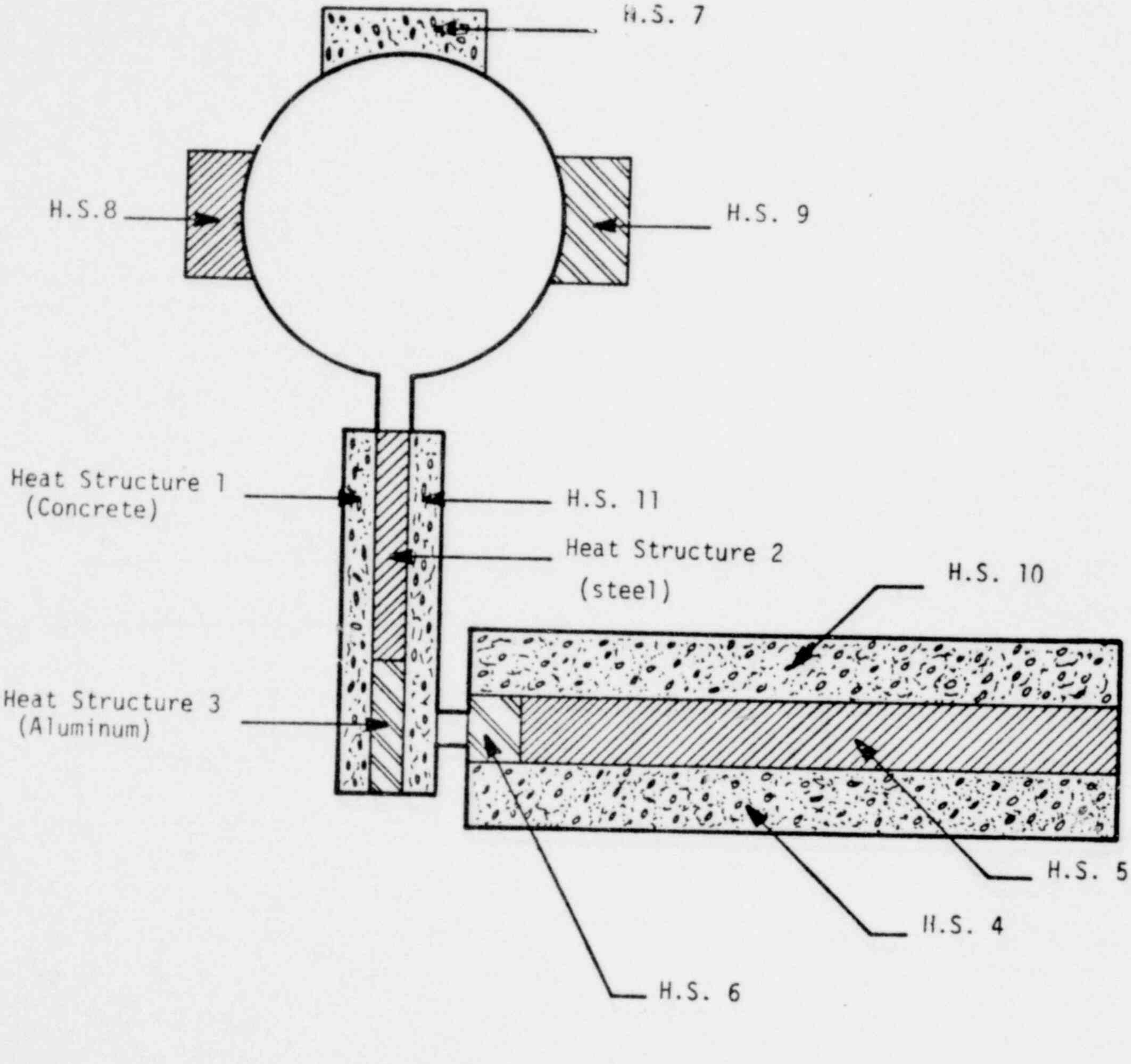

Fig. 28 Heat structure arrangement for Sample Problem 7 showing location of each material present.

```
100     "SAMPLE PROBLEM 7:  DRY MULTI-COMPARTMENT CONTAINMENT"
110     0.0, 0.50, .0001, SEC, 10., 1,    XEQ
120     0.004, 0.02, 0.02, 0.10, 0.05, 1.00, 0.10, 5.00
130     AUTODT,  000, 0.1, 2.0
140     PRINT, NOPRINT, PRINT,NOPRINT, NOPRINT, 99999
150     PLOTS, 0.9, 1, 1, 0, 0, 0, 0, 0, 0, 0, 1, 0, 0, 1, 1
160     MULTI, VARI, NOFLOPT
170     4, 1, 1, 4
180     1, 0.001
200     1.0, 0.0001, 0.0001, 300, 5, 10
210     -9.8, M, SEC-2, 0.02, 0.38, BTU/HR-FT-DEGF, 1.0E5
220     4.5E-4, 5.0E-6, FT2/SEC, 1., 0.1, MM, 125., MM3, 1.E5, 1
230     1, 0.001, 0.001
240     LASL, PT, BAR, DEGC, M, SEC-1
*******DEFAULT WALL FILM PARAMETERS ON FOLLOWING CARD*********
250     0.01, 0.0075, 0.9, 0.6, 2.75E-05, 0.7, 0.07
*******MESH DIMENSIONS AND INITIAL CONDITIONS
11000   CARTSN, 6, 3, 0.98, .85, 1.65, M, 0., 1.
*******THE FOLLOWING CARD DESCRIBES VARIABLE DR DIMENSION****
*******FOR MESH 1                ********************************
11020   0.8, 1.2, 1.5, 1.8, 2.0, 2.5
21000   CARTSN, 1, 1, .49, .5183, .5183, M, 0., 1.
31000   CARTSN, 3, 4, .47, 0.94, 1.65, M, 0., 1.
*******THE FOLLOWING CARD DESCRIBES VARIABLE DZ DIMENSION****
*******FOR MESH 3                ********************************
31030   2.0, 1.5, 1.2, 0.94
41000   CARTSN, 1, 1, .5183, 1.0, 0.5183, M, 0., 1.
*  NOTE:  FLOW LENGTH OF 1X1 1-D MESHES ARE TWICE THAT
*         USED IN THE FINE NODALIZATION CASE
11101   MIXTURE, 2, 2, 7, 4, 0, 1., 13.2, 13.2, 1.000, 0.9925
21101   MIXTURE, 2, 2, 2, 2, 0, 1., 13.2, 13.2, 1.000, 0.9925
31101   MIXTURE, 2, 2, 4, 5, 0, 1., 13.2, 13.2, 1.000, 0.9925
*******NEXT TWO CARDS ARE TO ACTIVATE WALL FILM MODEL*******
41101   MIXTURE, 2, 2, 2, 2, 0, 1., 13.2, 13.2, 1.000, 0.9925
11050   FILM
31050   FILM
*******LUMPED PARAMETER REGION MODELING
12000   ZERUD, 560.76, M3, 1.E4, 0.001, 0.001
12010   MIXTURE, 1., 13.2, 13.2, 1.000, 0.9925
*******BREAK MODELING
3010    STEAM, 1, 7, 4, 3011
3011    SEC, KG/SEC, J/GM, M, SEC-1
3012    .000, 0.0,   2774.1, 0.
3013    .007, 0.0,   2774.1, 0.
3014    .020, 72.4,  2774.1, 0.
3015    .050, 84.6,  2774.1, 0.
3016    .075, 86.6,  2774.1, 0.
3017    .100, 82.4,  2774.1, 0.
3018    .200, 71.4,  2774.1, 0.
3019    .300, 57.6,  2774.1, 0.
3020    .500, 49.9,  2774.1, 0.
3021    1.00, 45.3,  2774.1, 0.
3022    1.50, 43.1,  2774.1, 0.
3023    2.00, 41.4,  2774.1, 0.
3024    3.00, 36.8,  2774.1, 0.
6001    LEFT, 1, 2, 3, 1, 2, 2, 2, 1
6002    LEFT, 2, 2, 2, 1, 3, 4, 2, 1
6003    TOP, 3, 3, 5, 1, 4, 2, 2, 1
7001    TOP, 4, 2, 2, 1, 1.0
```

Fig. 29 Input card listing for Sample Problem 7.

```
*******THE REMAINING DATA CARDS ACTIVATE AND DESCRIBE*********
*******HEAT STRUCTURE MODEL                           *********
1000001        FT, BTU/HR, DEGK
1000002        -1    SEC     0.001
1000000        BTU/HR-FT-DEGF,  BTU/FT3-DEGF,  BTU/HR-FT2-DEGF
*                CONCRETE            STEEL           ALUMINUM
1000101        1.00    33.02    30.05    55.01    119.00    35.48
1010000       'ROOM 4 (MESH 3), LEFT CONCRETE'
1010001        6  1  0.0  0.0  100  0.01  0
1010002        MULTI  3  2  2  2  5  LUMPED  1  0  0  0  0
1010003        FT2,  415.7,  FACES, NONE
1010009        11  11  11  11
1010200        0  2
1010201        .1667  5
1010301        1  5
1010401        0.0  5
1010601        286.35  6
1020000       'ROOM 4 (MESH 3), STEEL'
1020001        3  1  0.0  0.0  100  0.01  0
1020002        MULTI  3  3  3  3  5  DUMMY   0  0  0  0  0
1020003        FT2, 340.88, FACES, NONE
1020009        11  11   0   0
1020200        0  2
1020201        .007  2
1020301        2  2
1020401        0.0  2
1020601        286.35  3
1030000       'ROOM 4 (MESH 3), ALUMINUM'
1030001        3  1  0.0  0.0  100  0.01  0
1030002        SINGLE 3  3  2  0  0  DUMMY   0  0  0  0  0
1030003        FT2, 12.92, FACES, NONE
1030009        11  11   0   0
1030200        0  2
1030201        .009  2
1030301        3  2
1030401        0.0  2
1030601        286.35  3
1040000       'ROOM 6 (MESH 1), LOWER CONCRETE'
1040001        6  1  0.0  0.0  100  0.01  0
1040002        MULTI   1  2  2  7  2  LUMPED  1  0  0  0  0
1040003        FT2,  484.61, FACES, NONE
1040009        11  11  11  11
1040200        0  2
1040201        .1667  5
1040301        1  5
1040401        0.0  5
1040601        286.35  6
1050000       'ROOM 6 (MESH 1), STEEL'
1050001        3  1  0.0  0.0  100  0.01  0
1050002        MULTI   1  3  3  7  3  DUMMY   0  0  0  0  0
1050003        FT2, 450.84, FACES, NONE
1050009        11  11   0   0
1050200        0  2
1050201        .009  2
1050301        2  2
1050401        0.0  2
1050601        286.35  3
1060000       'ROOM 6 (MESH 1), ALUMINUM'
1060001        3  1  0.0  0.0  100  0.01  0
1060002        SINGLE  1  2  3  0  0  DUMMY   0  0  0  0  0
1060003        FT2, 102.22, FACES, NONE
1060009        11  11   0   0
1060200        0  2
1060201        .010  2
1060301        3  2
1060401        0.0  2
1060601        286.35  3
```

```
1070000        'ROOM 9 (LPR 1), CONCRETE'
1070001          6  1  0.0  0.0  100  0.01  0
1070002          LUMPED  1  0  0  0  0  DUMMY   0  0  0  0  0
1070003          FT2, 9581.87, NONE, NONE
1070009          11  11   0   0
1070200          0  2
1070201          .1667  5
1070301          1  5
1070401          0.0  5
1070601          286.35  6
1080000        'ROOM 9 (LPR 1), STEEL'
1080001          3  1  0.0  0.0  100  0.01  0
1080002          LUMPED  1  0  0  0  0  DUMMY   0  0  0  0  0
1080003          FT2, 3432.66, NONE, NONE
1080009          11  11   0   0
1080200          0  2
1080201          .005  2
1080301          2  2
1080401          0.0  2
1080601          286.35  3
1090000        'ROOM 9 (LPR 1), ALUMINUM'
1090001          3  1  0.0  0.0  100  0.01  0
1090002          LUMPED  1  0  0  0  0  DUMMY   0  0  0  0  0
1090003          FT2, 218.44, NONE, NONE
1090009          11  11   0   0
1090200          0  2
1090201          .009  2
1090301          3  2
1090401          0.0  2
1090601          286.35  3
1100000        'ROOM 6 (MESH 1), UPPER CONCRETE'
1100001          6  1  0.0  0.0  100  0.01  0
1100002          MULTI   1  2  4  7  4  LUMPED  1  0  0  0  0
1100003          FT2,  484.61, FACES, NONE
1100009          11  11  11  11
1100200          0  2
1100201          .1667  5
1100301          1  5
1100401          0.0  5
1100601          286.35  6
1110000        'ROOM 4 (MESH 3), RIGHT CONCRETE'
1110001          6  1  0.0  0.0  100  0.01  0
1110002          MULTI  3  4  2  4  5  LUMPED  1  0  0  0  0
1110003          FT2,  415.7,  FACES, NONE
1110009          11  11  11  11
1110200          0  2
1110201          .1667  5
1110301          1  5
1110401          0.0  5
1110601          286.35  6
.
```

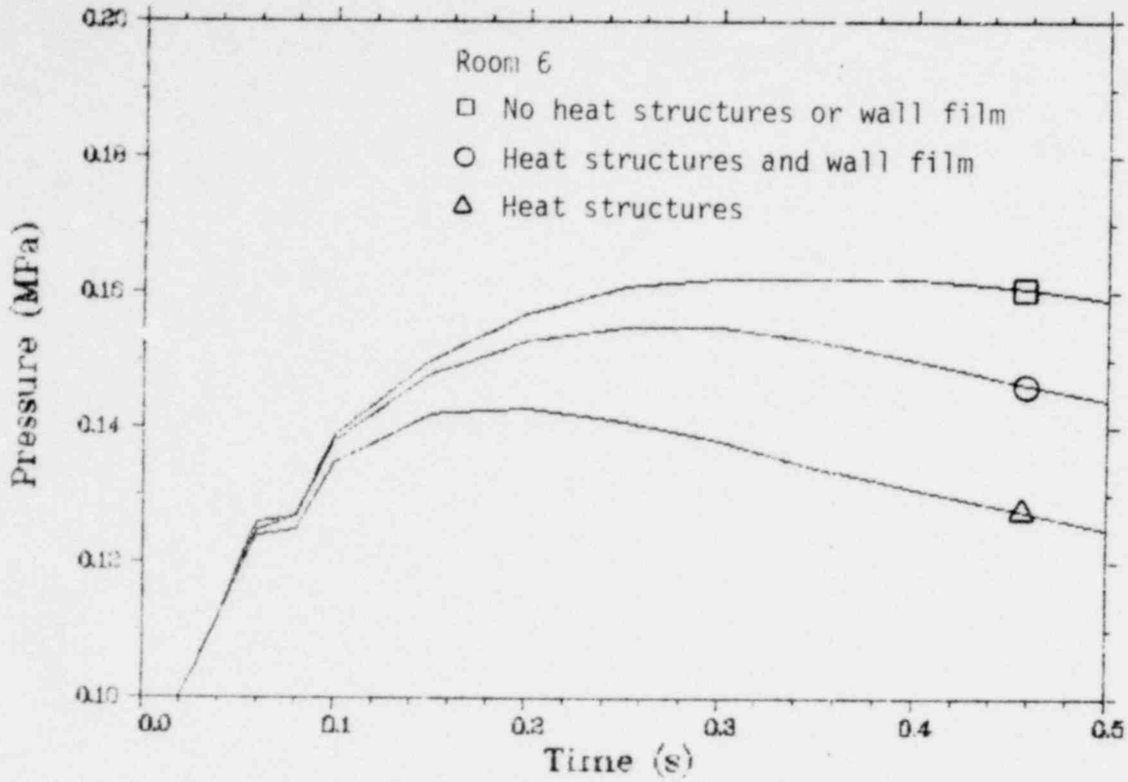

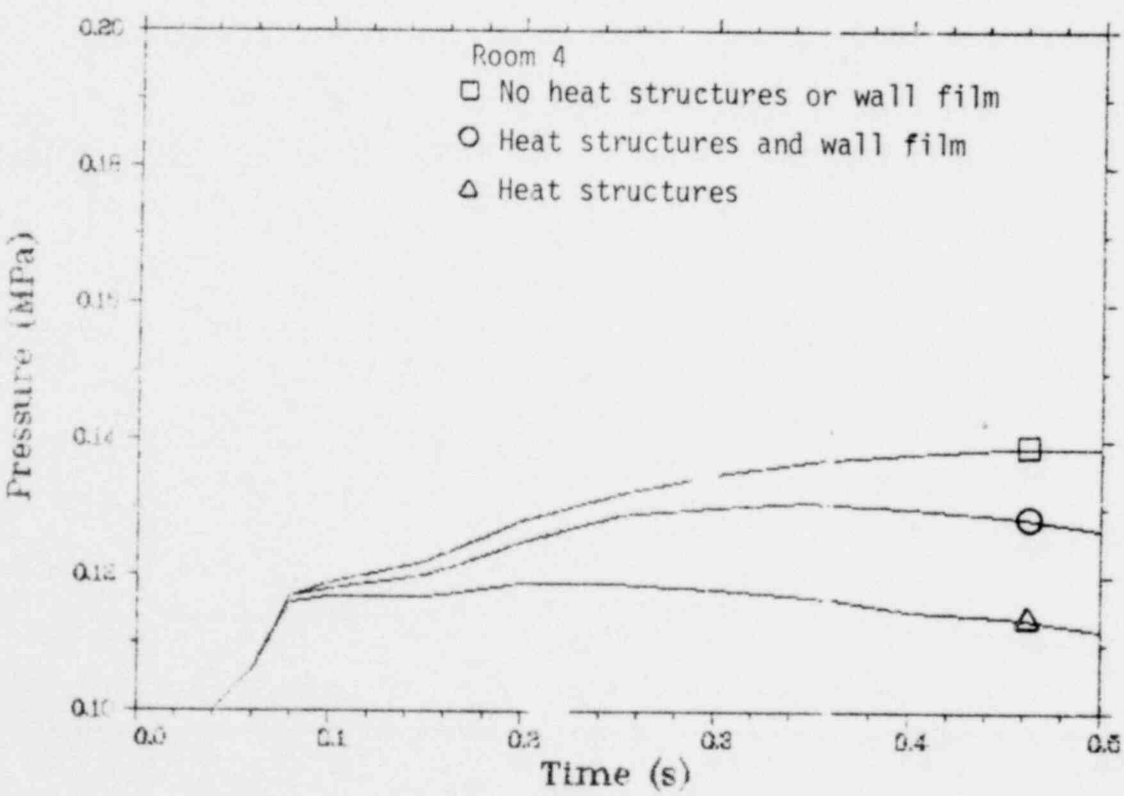

Fig. 30 Effects of wall film and heat structure modeling on pressures calculated near the centers of Rooms 6 and 4.

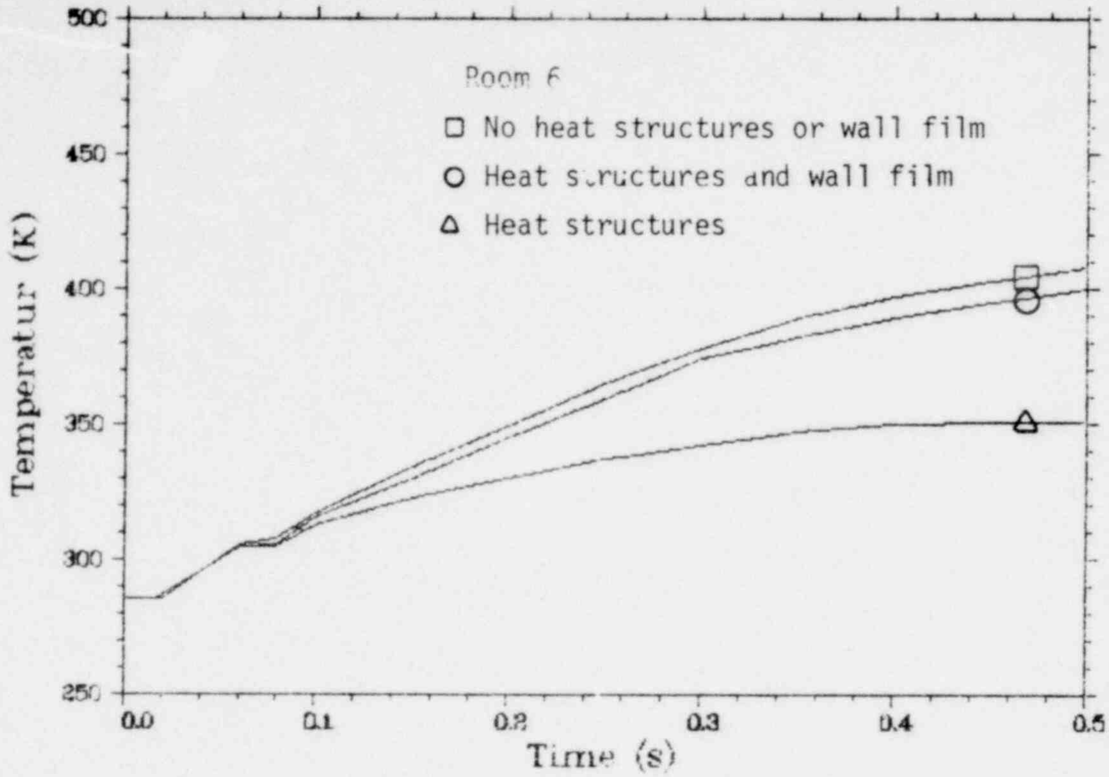

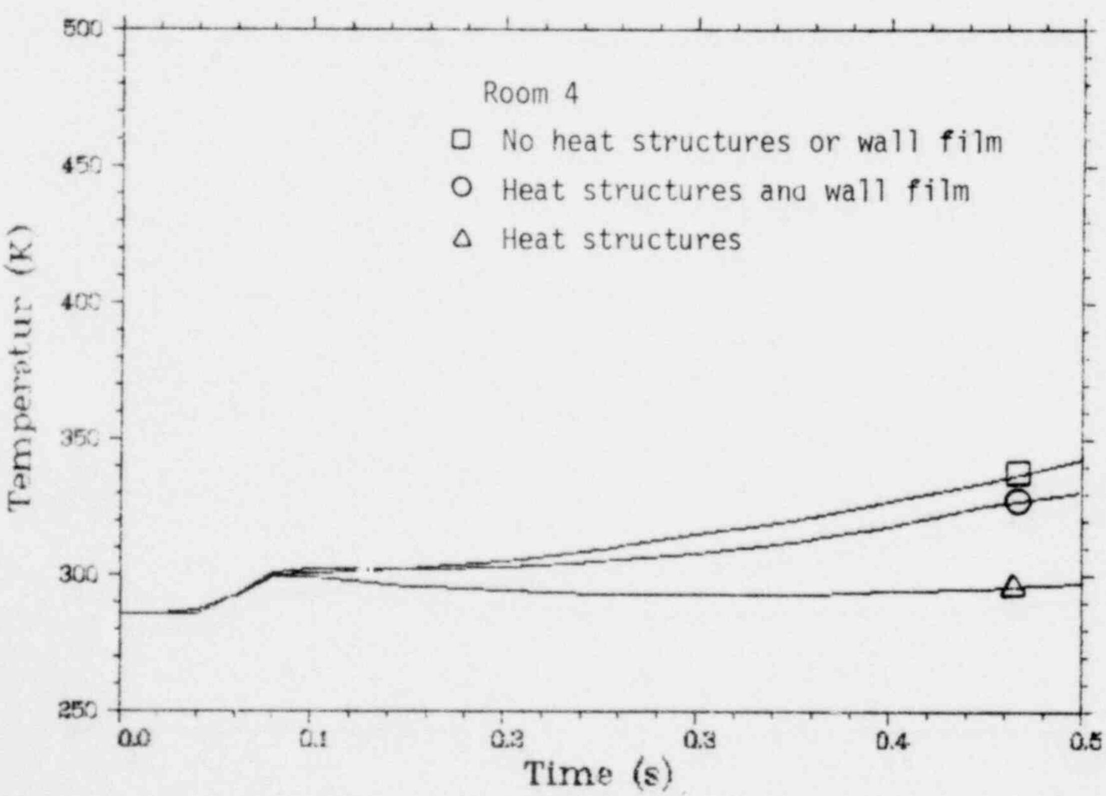

Fig. 31 Effects of wall film and heat structure modeling on temperatures calculated near the centers of Rooms 6 and 4.

SAMPLE PROBLEM 7   DRY CONTAINMENT MULTI-COMPARTMENT PROBLEM

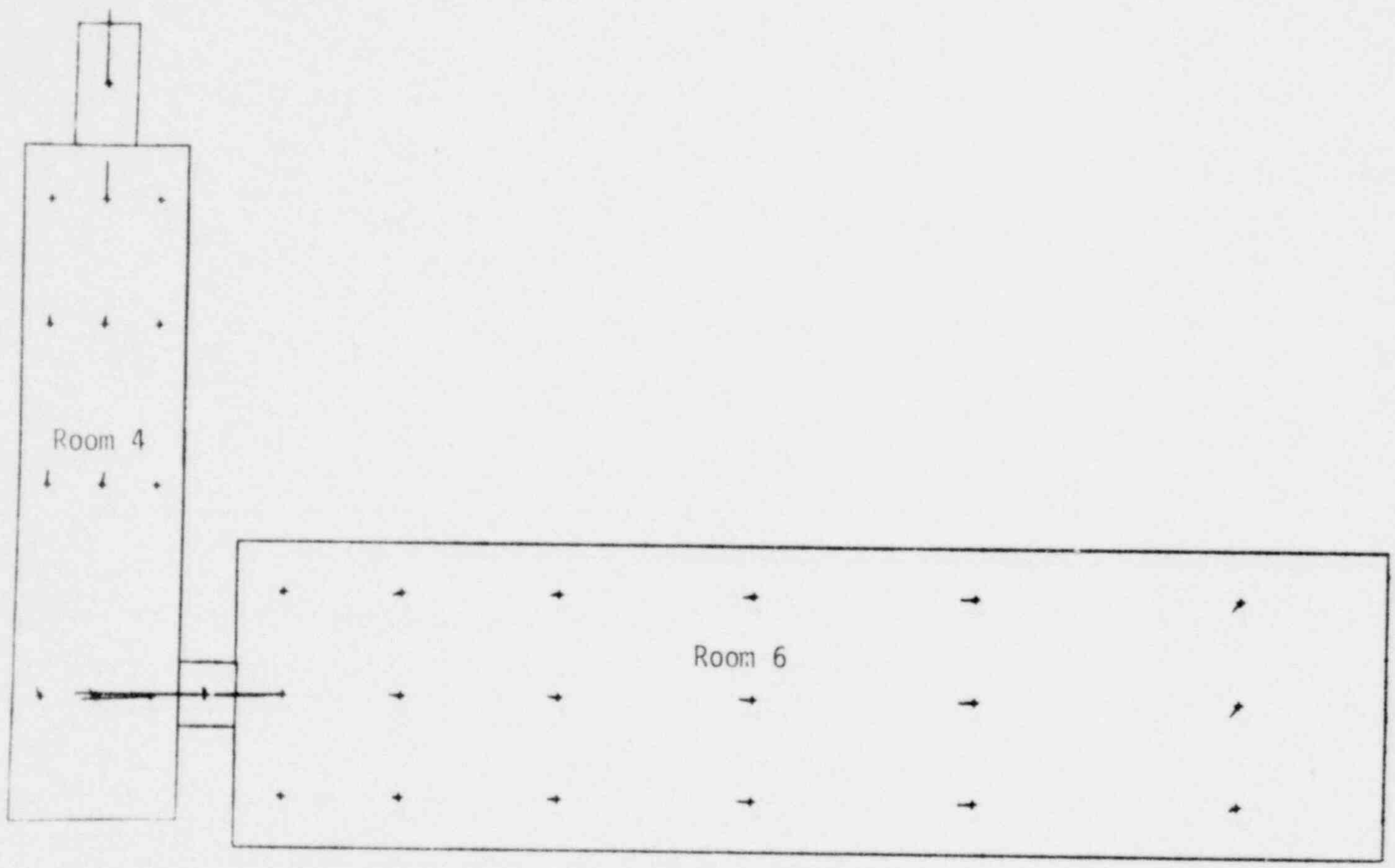

VAPOR.
TIME= 8.000-02   CYCLE= 173   MAXIMUM VELOCITY = 1.91513+02
MESH= 3   GEOM= CARTSN   JNM= JARTBXF

Fig. 32 Composite of BEACON vapor velocity vector plots for Sample Problem 7 showing relative magnitudes and directions near the time of maximum inflow of steam.

SAMPLE PROBLEM 7   DRY CONTAINMENT MULTI-COMPARTMENT PROBLEM

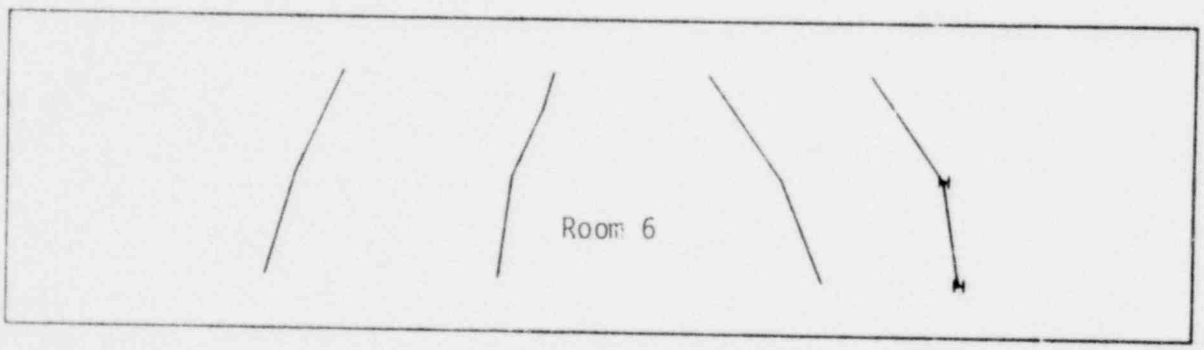

PRESSURE
TIME= 8.000-02 CYCLE= 173 MESH= 1 GEOM= CARTSN JNM= JARTBXF
MIN= 1.150+05 MAX= 1.339+05 L= 1.150+05 H= 1.320+05 DQ= 1.886+03

Fig. 33 Contour plot for Sample Problem 7 showing pressure gradient in Room 6 near the time of maximum steam inflow.

SAMPLE PROBLEM 7   DRY CONTAINMENT MULTI-COMPARTMENT PROBLEM

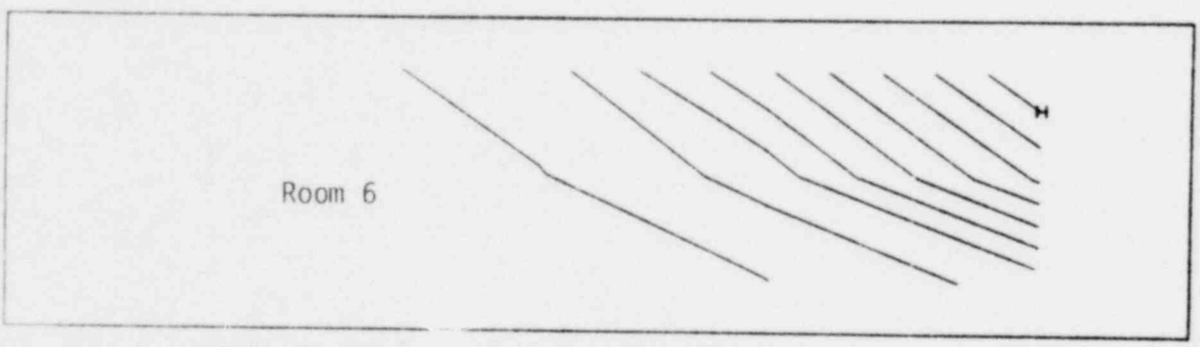

TGAS

TIME= 8.000-02   CYCLE= 173   MESH= 1   GEOM= CARTSN   JNM= JARTBXF

MIN= 2.980+02   MAX= 4.289+02   L= 2.980+02   H= 4.158+02   DQ= 1.309+01

Fig. 34 Contour plot for Sample Problem 7 showing temperature gradient in Room 6 near the time of maximum steam inflow.

SAMPLE PROBLEM 7   DRY CONTAINMENT MULTI-COMPARTMENT PROBLEM

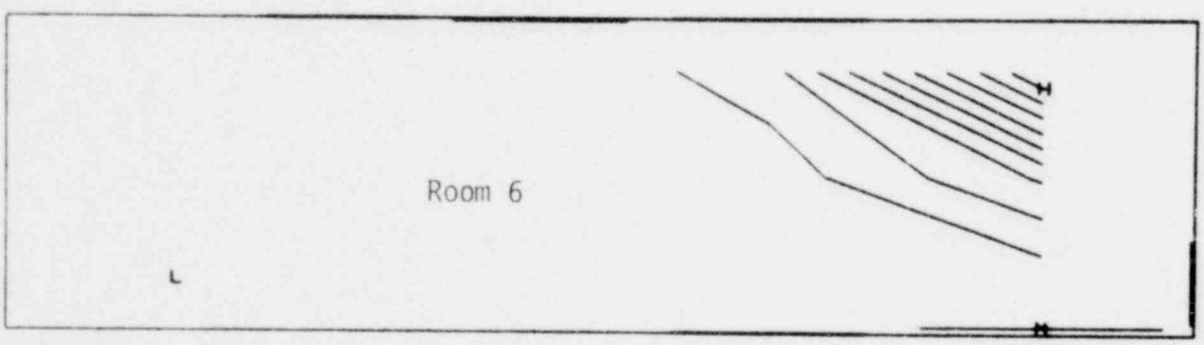

FMASS   MAX. 1-D FILM MASS = M =   1.732-06
TIME= 8.000-02   CYCLE= 173   MESH= 1   GEOM= CARTS'N   JNM= JARTBXF
MIN= 0.000   MAX= 4.471-03   L= 0.000   H= 4.024-03   DQ= 4.471-04

Fig. 35 Contour plot for Sample Problem 7 showing large concentration of film mass near the steam source and on the floor of Room 6 near the time of maximum steam inflow.

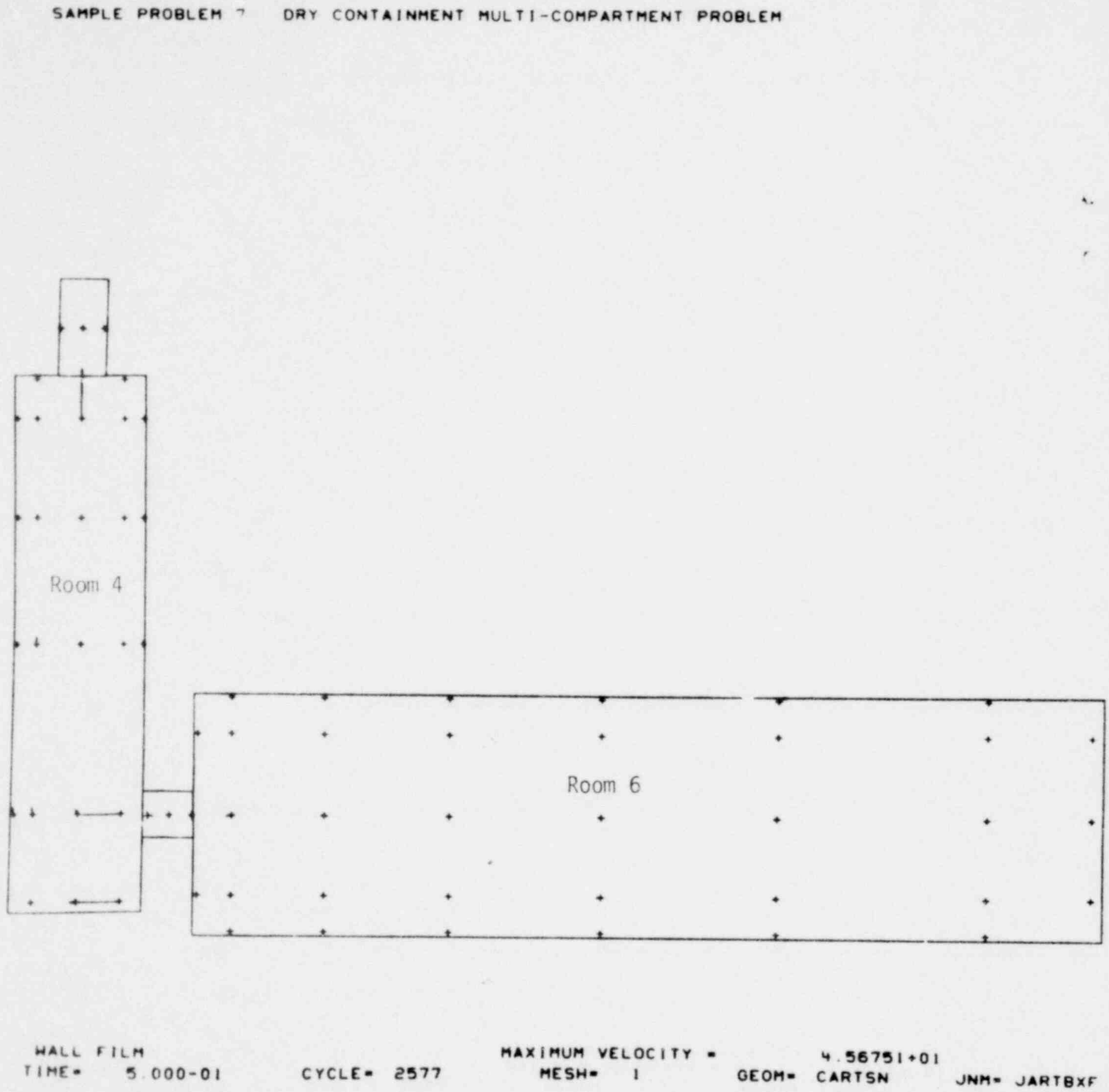

Fig. 36 Film velocity vector plot for Sample Problem 7 showing relative magnitudes and directions later in the problem.

SAMPLE PROBLEM 7   DRY CONTAINMENT MULTI-COMPARTMENT PROBLEM

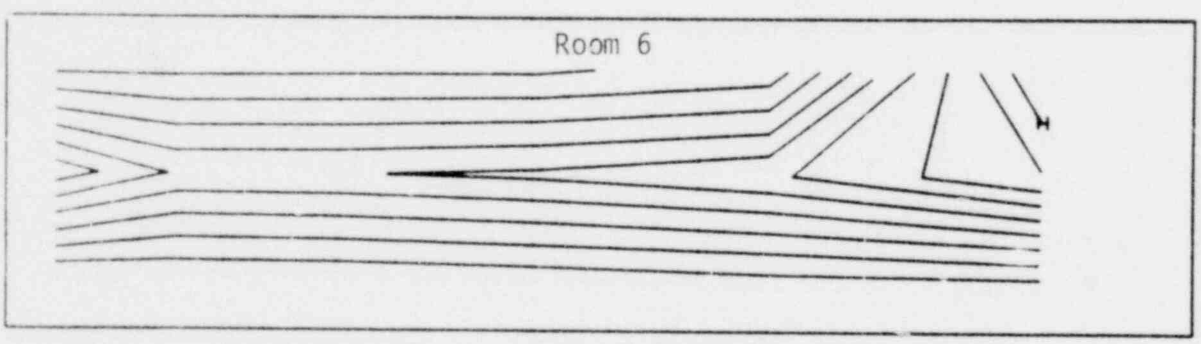

FTEMP
TIME= 5.000-01   CYCLE= 2577   MESH= 1   GEOM= CARTSN   JNM= JARTBXF
MIN= 2.865+02   MAX= 3.068+02   L= 2.865+02   H= 3.048+02   DQ= 2.033+00

Fig. 37 Contour plot for Sample Problem 7 showing film temperature variation throughout Room 6 later in the problem.

III. CONCLUSIONS

Seven sample problems, designed to investigate different code models and options, were run with BEACON/MOD2A. By rerunning five standard sample problems, it was determined that no obvious errors were introduced into the new MOD2A version of the code. Several new code capabilities (partial flow, variable mesh, wall film, and heat structures) were checked out by running two additional problems. The calculations all indicate that physical phenomena appear to be handled properly and that the answers seem to be correct.

For the most complex problem (the dry, multi-compartment containment case with wall film and heat structures),a comparison was made to investigate the increase in computer time required to handle the new heat structure and wall film routines. The addition of only the heat structure modeling increased CPU time by about 9%, while the addition of both heat structure and wall film calculations required a 50% increase in run time. However, this single example of increased computing time using the film option is not necessarily representative of all problems modeled with BEACON. This problem was not intended for quantitative comparisons, however, the respective lowered temperatures and pressures illustrated expected behavior.

The results of checkout of the code indicate that all of the models are operating satisfactorily. The calculations seem to give accurate answers and there are no unusual effects or gross deviations from expected physical trends. In conclusion, BEACON/MOD2A appears to be ready for public release.